Circulation Research

ORIGINAL RESEARCH

CaMKIIδC Drives Early Adaptive Ca^{2+} Change and Late Eccentric Cardiac Hypertrophy

Senka Ljubojevic-Holzer, Anthony W. Herren, Natasa Djalinac, Julia Voglhuber[iD], Stefano Morotti, Michael Holzer, Brent M. Wood, Mahmoud Abdellatif, Ingrid Matzer[iD], Michael Sacherer, Snjezana Radulovic, Markus Wallner, Milan Ivanov, Stefan Wagner[iD], Samuel Sossalla, Dirk von Lewinski, Burkert Pieske, Joan Heller Brown, Simon Sedej[iD], Julie Bossuyt, Donald M. Bers[iD]

RATIONALE: CaMKII (Ca^{2+}-Calmodulin dependent protein kinase) δC activation is implicated in pathological progression of heart failure (HF) and CaMKIIδC transgenic mice rapidly develop HF and arrhythmias. However, little is known about early spatio-temporal Ca^{2+} handling and CaMKII activation in hypertrophy and HF.

OBJECTIVE: To measure time- and location-dependent activation of CaMKIIδC signaling in adult ventricular cardiomyocytes, during transaortic constriction (TAC) and in CaMKIIδC transgenic mice.

METHODS AND RESULTS: We used human tissue from nonfailing and HF hearts, 4 mouse lines: wild-type, KO (CaMKIIδ-knockout), CaMKIIδC transgenic in wild-type (TG), or KO background, and wild-type mice exposed to TAC. Confocal imaging and biochemistry revealed disproportional CaMKIIδC activation and accumulation in nuclear and perinuclear versus cytosolic regions at 5 days post-TAC. This CaMKIIδ activation caused a compensatory increase in sarcoplasmic reticulum Ca^{2+} content, Ca^{2+} transient amplitude, and [Ca^{2+}] decline rates, with reduced phospholamban expression, all of which were most prominent near and in the nucleus. These early adaptive effects in TAC were entirely mimicked in young CaMKIIδ TG mice (6–8 weeks) where no overt cardiac dysfunction was present. The (peri)nuclear CaMKII accumulation also correlated with enhanced HDAC4 (histone deacetylase) nuclear export, creating a microdomain for transcriptional regulation. At longer times both TAC and TG mice progressed to overt HF (at 45 days and 11–13 weeks, respectively), during which time the compensatory Ca^{2+} transient effects reversed, but further increases in nuclear and time-averaged [Ca^{2+}] and CaMKII activation occurred. CaMKIIδ TG mice lacking δB exhibited more severe HF, eccentric myocyte growth, and nuclear changes. Patient HF samples also showed greatly increased CaMKIIδ expression, especially for CaMKIIδC in nuclear fractions.

CONCLUSIONS: We conclude that in early TAC perinuclear CaMKIIδC activation promotes adaptive increases in myocyte Ca^{2+} transients and nuclear transcriptional responses but that chronic progression of this nuclear Ca^{2+}-CaMKIIδC axis contributes to eccentric hypertrophy and HF.

GRAPHIC ABSTRACT: A graphic abstract is available for this article.

Key Words: calcium ▪ CaMKII ▪ heart failure ▪ hypertrophy ▪ mice

---

Meet the First Author, see p 1121

Development of hypertrophy and its progression to heart failure (HF) is characterized by altered cardio-myocyte Ca^{2+}, excitation-contraction coupling (ECC), and the activation of multiple Ca^{2+}-linked hypertrophic signaling pathways, a process referred to as excitation-transcription coupling (ETC).[1,2] Better understanding of the mechanisms leading to abnormal Ca^{2+} cycling in pathology may lead to novel and effective therapeutic strategies.

Circulation Research is available at www.ahajournals.org/journal/res

Novelty and Significance

What Is Known?

- Transcriptional changes and reactivation of fetal gene programs are hallmark of hypertrophic cardiac remodeling and progression to heart failure.
- CaMKII (Ca²⁺-Calmodulin dependent protein kinase) is a nodal regulator of diverse acute and long-term signaling to downstream cellular targets.
- CaMKII activation is implicated in heart failure progression and transgenic overexpression of cardiac CaMKIIδC rapidly induces heart failure and arrhythmias.

What New Information Does This Article Contribute?

- Using multiple mouse models to study early cardiac hypertrophy we found disproportional CaMKIIδ activation in the nuclear and perinuclear versus cytosolic region.
- Early in pressure overload (transaortic constriction) and CaMKIIδC overexpression, perinuclear CaMKII activation enhanced Ca²⁺ cycling and sarcoplasmic reticulum Ca²⁺ uptake as an adaptive response to pressure overload.
- Later, chronic CaMKIIδC activation leads to its nuclear accumulation and drives maladaptive transcriptional effects, eccentric cardiac hypertrophy, and progression to heart failure.

The hypertrophied and failing heart exhibits abnormalities in signal transduction systems, and CaMKIIδ has emerged as a key nodal promoter of cardiac remodeling. This article provides new mechanistic insight into how isoform-specific CaMKIIδ activation can drive early adaptive Ca²⁺ handling changes to help meet hemodynamic demands while also causing later maladaptive cardiac alterations. While CaMKIIδ post-translational modifications in the regulatory domain have been identified and associated with various cardiac pathologies, here we describe, for the first time that (peri)nuclear accumulation of activated CaMKIIδC is a critical step in the development and progression of eccentric cardiac growth. Also, we provide first functional evidence that perinuclear region is a fine-tuned microdomain for transcriptional regulation serving as a local pool of Ca²⁺-dependent transcription factors that are poised for shuttling in and out of the nucleus when local [Ca²⁺] is elevated. Importantly, using human tissue from nonfailing and failing hearts we showed that these findings extend to humans and may have clinical relevance. This may open new avenues for therapeutic strategies that can—by acting on a subset of downstream targets—improve efficacy and minimize off-target effects that can accompany nonselective CaMKIIδ inhibition.

Nonstandard Abbreviations and Acronyms

[Ca]Cyto	cytoplasmic [Ca²⁺]
[Ca]Nuc	nuclear [Ca²⁺]
CaMKII	Ca²⁺-Calmodulin dependent protein kinase II
CaT	Ca²⁺ transient
ECC	excitation-contraction coupling
ETC	excitation-transcription coupling
HDAC	histone deacetylase
HF	heart failure
IL6R	interleukin-6 receptor
KN-93	N-[2-[[[(E)-3-(4-chlorophenyl) prop-2-enyl]-methylamino]methyl] phenyl]-N-(2-hydroxyethyl)-4-methoxy-benzenesulfonamide
KO	CaMKIIδ-knockout
KO-δCTG	CaMKIIδC transgenic in KO background
NE	nuclear envelope
PKA	protein kinase A
PKD	protein kinase D
PLB	phospholamban
PN	perinuclear region
RyR	ryanodine receptor
SERCA	SR Ca²⁺-ATPase
SR	sarcoplasmic reticulum
TAC	transaortic constriction
TGF-ß1	transforming growth factor-ß1
WT	wild type

At each beat, the cytosolic Ca²⁺ transient (CaT) that drives cardiomyocyte contraction and relaxation also drives nuclear CaT.[3] However, the nuclear envelope (NE) slows the kinetics and reduces the amplitude of nucleoplasmic versus cytoplasmic CaT. Indeed, normally nuclear CaTs appear to depend mainly on Ca²⁺ diffusion into and out of the nucleus via nuclear pores, with most sarcoplasmic reticulum (SR) Ca²⁺ release and reuptake occurring outside the nucleus.[4] Abnormal myocyte Ca²⁺ handling may be an early event in myocardial remodeling, and signaling via CaMKII (Ca²⁺-Calmodulin dependent protein kinase) has been shown to alter both cytosolic ECC and nuclear ETC[1,5] The slower nuclear [Ca²⁺] ([Ca]$_{Nuc}$) decline

causes progressive elevation of diastolic $[Ca]_{Nuc}$ at higher pacing rates and this elevated $[Ca]_{Nuc}$ is exacerbated in HF, in part because of altered nuclear structure and nuclear pore location.[4] This makes nuclear Ca^{2+} handling of particular interest for Ca^{2+}-dependent ETC and altered protein expression in the progression of hypertrophy and its transition to HF. Yet, there is a need for more detailed information as to how nuclear versus cytosolic CaMKIIδ (the predominant cardiac isoform) gets activated during the progression toward HF and how that modulates HDAC (histone deacetylase) nuclear export which regulates transcription.

Two key CaMKIIδ splice variants, CaMKIIδB and CaMKIIδC, differ by only an 11 amino acid nuclear localization signal in the former. While CaMKIIδB tends to be more nuclear than CaMKIIδC, both variants exist in nucleus and cytosol[6] and were found to be remarkably mobile within the myocyte, especially upon activation.[7] Acute CaMKIIδC effects are mediated by direct modulation of non-nuclear proteins, such as RyRs (ryanodine receptors), L-type Ca^{2+} channels, PLB (phospholamban), ion channels, and myofilaments, to mediate contractile dysfunction and arrhythmogenesis.[5] Conversely, CaMKIIδB is thought to control transcriptional CaMKII effects on gene-regulating proteins (eg, HDACs). But detailed examination of CaMKIIδ localization revealed more spatial overlap and that CaMKIIδC is more pathological, while CaMKIIδB may restrain the negative effects of CaMKIIδC.[6,8]

Here, we used 4 mouse lines: wild-type (WT), CaMKIIδC transgenic (TG), KO (CaMKIIδ-knockout), or CaMKIIδC transgenic in the KO background (KO-δCTG). We also exposed WT mice to transaortic constriction (TAC) to study early hypertrophy and HF, stages where CaMKIIδ expression and activation are elevated. We found overproportional CaMKII activation in the nuclear and perinuclear versus cytosolic region. Notably, these effects were mainly due to CaMKIIδC and not the more nuclear CaMKIIδB and correlated with effects on HDAC4 nuclear export. Human samples confirmed the more prominent nuclear CaMKIIδC expression in HF. Moreover, we found that nuclear CaMKIIδC activation and HDAC4 nuclear export were already apparent in both young CaMKIIδC-TG and TAC mice far before signs of HF were evident. Finally, elevated CaMKIIδC promoted eccentric cardiac growth, leading to accelerated chamber dilation, without adaptive hypertrophy of the ventricular wall. Thus, we provide clear evidence for early activation of the CaMKIIδC axis during TAC and subsequent CaMKIIδC-dependent enhancement of nuclear Ca^{2+} signaling which further promotes the activation and (peri)nuclear accumulation of CaMKIIδC. The autoreinforcing property of CaMKIIδC signaling may be critical in the progression from hypertrophy to HF via the interplay of ECC and ETC.

METHODS

The data supporting findings of this study are available from the corresponding author upon reasonable request. Materials and methods are described in detail in the Data Supplement. All essential research materials are listed in the Major Resources Table in the Data Supplement.

All procedures involving animals adhered to the National Institutes of Health Guide for the Care and Use of Laboratory Animals (UC Davis) or the Federal Act on the Protection of Animals (Medical University of Graz) and were approved by the Institutional Animal Care and Use Committee. Human sample use was approved by the Ethical Committee of the Medical University of Graz and was carried out in accordance with the Declaration of Helsinki. Patient characteristics are summarized in Table I.

RESULTS

Larger Cytoplasmic and Nuclear CaTs Early in TAC Are CaMKII-Dependent

Fluo-4 fluorescence signals recorded during electrical stimulation were transformed into cytoplasmic $[Ca^{2+}]$ ($[Ca]_{Cyto}$; black) and $[Ca]_{Nuc}$ (red) using our compartment-specific calibration methods (Figure 1A).[9,10] Sham-operated mice showed no statistical differences in CaTs between the 5- and 45-day groups and were pooled as one control group (for details on cardiac function see Table V in the Data Supplement). Early post-TAC (5 days) diastolic $[Ca]_{Cyto}$ was reduced, but $[Ca]_{Nuc}$ was unaltered (Figure 1B and 1D). CaT amplitudes were significantly increased ($\Delta[Ca]_{Cyto}$ by ≈45% and $\Delta[Ca]_{Nuc}$ by ≈80%; Figure 1C). Kinetics of both $[Ca]_{Cyto}$ and $[Ca]_{Nuc}$ decay were faster early in hypertrophy (Figure 1E), likely indicating faster SR Ca^{2+} uptake. Time to peak $[Ca]_{Nuc}$ (but not $[Ca]_{Cyto}$) was also shorter in early TAC (Figure 1F). Notably, the rise in CaT amplitude was more pronounced in the nucleus than cytosol (larger % change). We suggest that these early changes are mediated by enhanced SR Ca^{2+} uptake and release, as a compensation for the TAC-imposed afterload.

At the later HF stage (45 days post-TAC),[4] the diastolic [Ca] was elevated, and CaT amplitude was reduced in both cytosol and nucleus (Figure 1B through 1D), and the rate of [Ca] decline was slowed (Figure 1E). This is typical of CaT changes in HF.[4] Notably, the early phenotype in TAC-operated mice was associated already with persistent CaMKII activation, especially around NE (Figure 1G) and acute CaMKII inhibition by N-[2-[[[(E)-3-(4-chlorophenyl)prop-2-enyl]-methyl-amino]methyl]phenyl]-N-(2-hydroxyethyl)-4-methoxy-benzenesulfonamide (KN-93; Figure 1H and 1I), but not 2-[N-(4'-Methoxybenzenesulfonyl)]amino-N-(4'-chlorophenyl)-2-propenyl-N-methylbenzylamine phosphate (Figure I in the Data Supplement) could reverse the disturbed CaTs.
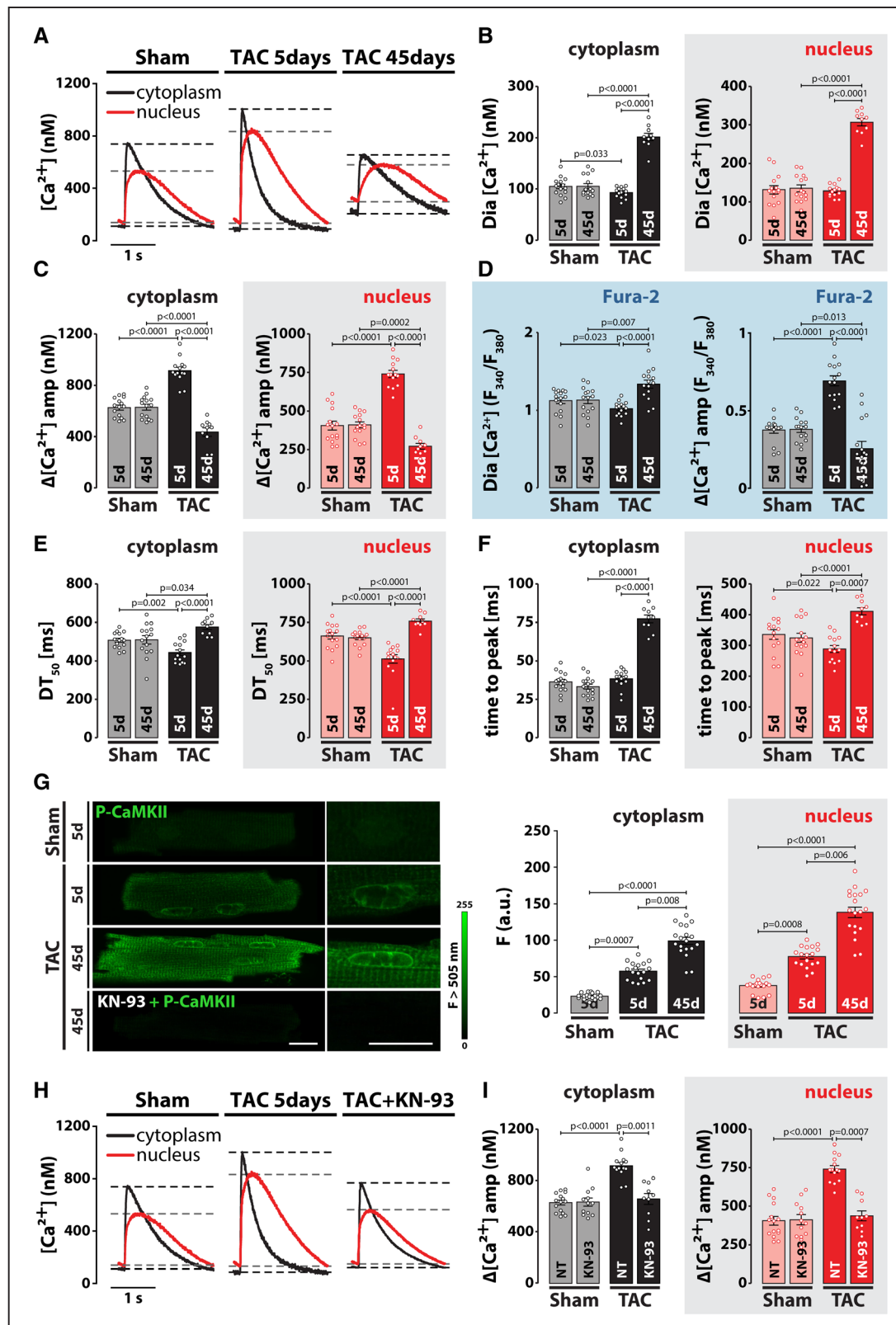
Figure 1. Characterization of cytoplasmic and nucleoplasmic [Ca²⁺] transients (CaTs) after pressure overload–induced hypertrophy and heart failure in mouse ventricular myocytes.

A, Averaged original recordings of electrically stimulated CaTs in the nucleus (red) vs cytoplasm (black) of cardiomyocytes from sham-operated mice (**left**) and from mice subjected to transaortic constriction (TAC) isolated 5 (**middle**) and 45 d (**right**) after intervention. **B**, Calibrated diastolic (Dia) [Ca²⁺] and (**C**) amplitude of nucleoplasmic (red) and cytoplasmic (black) CaTs. **D**, Diastolic (Dia) [Ca²⁺] corresponding to the global epifluorescence CaTs as measured by ratiometric Ca²⁺ indicator Fura-2. **E**, Time from peak [Ca²⁺] to 50% decline (DT₅₀) and (*Continued*)

Young CaMKIIδC Transgenic Mice Exhibit CaT Changes Like Those in Early TAC

Because mice transgenic for CaMKIIδC spontaneously develop hypertrophy and HF, we tested whether the TAC-induced changes were recapitulated in CaMKIIδC transgenic (TG) mice (Figure 2). Exactly as in early TAC, the 6- to 8-week CaMKIIδC-TG versus WT myocytes had lower diastolic $[Ca]_{Cyto}$, larger CaT amplitudes in cytosol and nucleus, and faster [Ca] decline in both compartments (Figure 2B through 2F). Also, as in early TAC, the percentage rise in $[Ca]_{Nuc}$ CaTs was higher than that for $[Ca]_{Cyto}$ in young TG myocytes versus WT. Conversely, in KO versus WT myocytes diastolic $[Ca]_{Cyto}$ and $[Ca]_{Nuc}$ were slightly elevated, $\Delta[Ca]_{Nuc}$ was lower, and the decay of $[Ca]_{Cyto}$ was slower. We conclude that at this early stage (like early TAC), CaMKIIδC overexpression elevates CaT amplitudes, and SR Ca^{2+} uptake mediated $[Ca]_{Cyto}$ decline. The KO versus WT results also suggest that even in WT a low level of CaMKIIδ-dependent SERCA (SR Ca^{2+}-ATPase) activation may promote larger and faster CaTs and limit diastolic $[Ca]_{Cyto}$ and $[Ca]_{Nuc}$.

A recent study by Baier et al[11] showed that excessive CaMKII inactivation in AC3-I (autocamtide-3-derived inhibitory peptide) transgenic mice impairs adaptation of ECC in early pressure-induced overload. Specifically, AC3-I transgenic mice fail to increase CaTs within 2 to 5 days after TAC, leading to diminished cardiac function and premature death, demonstrating that CaMKII activation is a pivotal part of cardiac stress physiology. To further test our finding that CaMKIIδC is exclusively responsible for early compensatory response, we measured CaTs from young CaMKIIδ transgenic mice with the genetic deletion of CaMKIIδ (KO-δCTG, Figure II in the Data Supplement). We found that 6-week-old KO-δCTG mice had increased CaTs and nucleoplasmic Ca^{2+} signaling, which resembled that of TG mice at the age between 6 and 8 weeks. Interestingly, we found a prominent reduction in nucleoplasmic but not cytoplasmic CaTs in 8-week-old KO-δCTG mice versus 6-week-old mice. This indicates that (1) KO-δCTG mice display accelerated remodeling as compared to TG mice, despite comparable CaMKII expression levels (Figure IIIA in the Data Supplement) and, (2) that CaMKIIδC causes Ca^{2+}-perturbations in the nucleus earlier than in the cytoplasm.

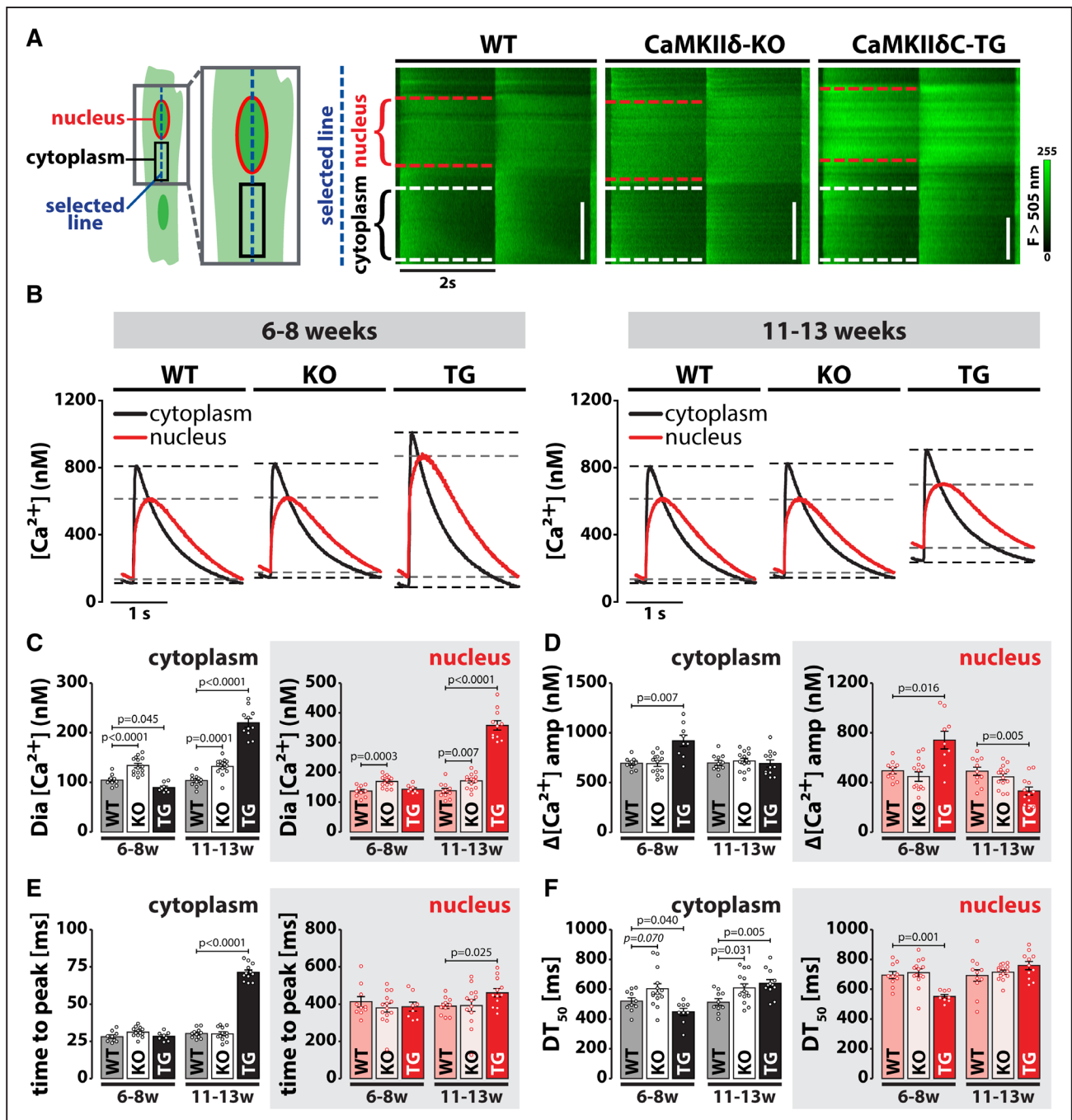As the CaMKIIδC-TG (CaMKIIδC transgenic mice) mice progress toward HF at 11 to 3 weeks of age, the CaT situation changes dramatically. At 11 to 13 weeks, TG mice (versus WT) have highly elevated diastolic $[Ca]_{Cyto}$ and $[Ca]_{Nuc}$, and slowed CaTs kinetics in both compartments, consistent with advanced remodeling with reprogrammed protein pattern. The $[Ca]_{Nuc}$ transient amplitude was greatly reduced, both versus WT and the 6- to 8-week data, but these nuclear CaTs were riding on a very large diastolic $[Ca]_{Nuc}$, such that peak $[Ca]_{Nuc}$ was above the WT, and time-averaged $[Ca]_{Nuc}$ was highly elevated (Figure 2B). The cytosolic CaT amplitude in 11- to 13-week TG mice was greatly reduced from that at 6 to 8 weeks but was still comparable to the WT $\Delta[Ca]_{Cyto}$. That differs from our early CaMKIIδC-TG mouse study in 2003,[12,13] where a ≈50% reduction in cytosolic CaT amplitude was seen at 12 weeks of age (and mice exhibited overt HF with nearly 50% mortality). However, it agrees with more recent studies in this TG line (2014)[14] where we found milder and delayed HF onset, with mortality beginning at 15 weeks. Thus, we infer that the 11- to 13-week TG mice in the present study are only at the onset of decompensating HF. Many disease-causing genetically modified mice develop less severe phenotype after many generations. It is not fully understood why, but one possibility is that it reflects a simple selective advantage of offspring that can better adapt to stresses, thereby limiting the strength of disease penetrance in subsequent generations.[15]

Increased SR Ca^{2+} Load and SERCA2/PLB Expression in Early TAC and Young CaMKIIδC Transgenic Mice

We next tested whether the faster [Ca] decline and elevated CaT amplitudes seen in early TAC and young CaMKIIδC-TG mice occurred with elevated SR Ca^{2+} content and whether it might be mediated by altered expression of SERCA2 and PLB. Figure 3A shows rapid caffeine-induced CaTs used to assess SR Ca^{2+} content, which was higher in early TAC mice whether measured in the cytosol or nucleus (Figure 2B). Fluo-4 is a high-affinity Ca^{2+} dye and caffeine-induced CaTs can reach the shallow nonlinear part of the calibration curve. Hence, we did not calibrate these values. The TAC-induced rise in SR Ca^{2+} load (ΔF) was larger in the nucleus versus cytosol (Figure 3B, right). The time constant of cytosolic $[Ca^{2+}]_i$ decline during the caffeine-induced Ca^{2+} transients was not statistically different between sham and 5-day TAC

Figure 1 Continued. (F) time to peak. **G,** Original confocal images (**left**) of cardiomyocytes from sham-operated and TAC-operated mice (5 and 45 d after intervention) immunostained for P-CaMKII (phospho-Ca^{2+}-Calmodulin dependent protein kinase) and average P-CaMKII fluorescence values (**right**) in nucleus vs cytoplasm. **H,** Averaged original recordings of electrically stimulated CaTs in the nucleus (red) vs cytoplasm (black) of cardiomyocytes from sham-operated (**left**) and TAC-operated mice in the absence (**middle**) and presence (**right**) of CaMKII inhibitor N-[2-[[[(E)-3-(4-chlorophenyl)prop-2-enyl]-methylamino]methyl]phenyl]-N-(2-hydroxyethyl)-4-methoxybenzenesulfonamide (KN-93). **I,** Corresponding calibrated amplitude of nucleoplasmic (red) and cytoplasmic (black) CaTs. **B** through **F**, n=10–15 myocytes per group. **G–I**, n=10–20 myocytes per group. *P* values were calculated using Mann-Whitney test comparing TAC, 45 d, or KN-93 to the respective control (**B–F**; I) or Kruskal-Wallis with Dunn post hoc test (**G**). Scale bars=20 µm. NT indicates normal tyrode.

Figure 2. Characterization of cytoplasmic and nucleoplasmic [Ca²⁺] transients (CaTs) in electrically stimulated ventricular myocytes isolated from 6- to 8-wk and 11- to 13-wk old CaMKIIδ-KO (Ca²⁺-Calmodulin dependent protein kinase δ knock out), wild-type (WT) and CaMKIIδC-TG mice.

A, Linescan imaging of cytoplasmic and nucleoplasmic CaTs in a cardiomyocyte. **B**, Averaged original recordings of distinct subcellular regions, as indicated in **A**: nucleus (red) vs cytoplasm (black) of cardiomyocytes from WT (**left**), CaMKIIδ-KO (KO, **middle**), and CaMKIIδC overexpressing mice (TG, **right**), isolated 6–8 or 11–13 wk after intervention. Diastolic (Dia) [Ca²⁺] (**C**), amplitude (**D**), time to peak (**E**) and time from peak [Ca²⁺] to 50% decline (DT$_{50}$) of nucleoplasmic (red) and cytoplasmic (black) CaTs. **B**–**E**, n=9–14 myocytes per group. *P* values were calculated using ANOVA with Dunnett post hoc test (**C** [6–8 wk], **E** and **F**), or Welch test with Dunnet T3 post hoc test (**C** [11–13 wk], **D**). Scale bars=10 µm.

(3.73±0.19 versus 3.75±0.21), suggesting unaltered Na⁺/Ca²⁺ exchange function at this early stage of hypertrophy.

We also analyzed the expression and activation of the key SR Ca²⁺ uptake proteins (SERCA2 and PLB) in left ventricular tissue lysates and isolated cardiomyocyte nuclei from control and TAC-operated mice 5 days post-TAC. SERCA2 levels were not significantly altered in either lysates or isolated nuclei at this stage, but PLB was significantly downregulated at 5 days post-TAC, whereas its phosphorylation was increased, resulting in
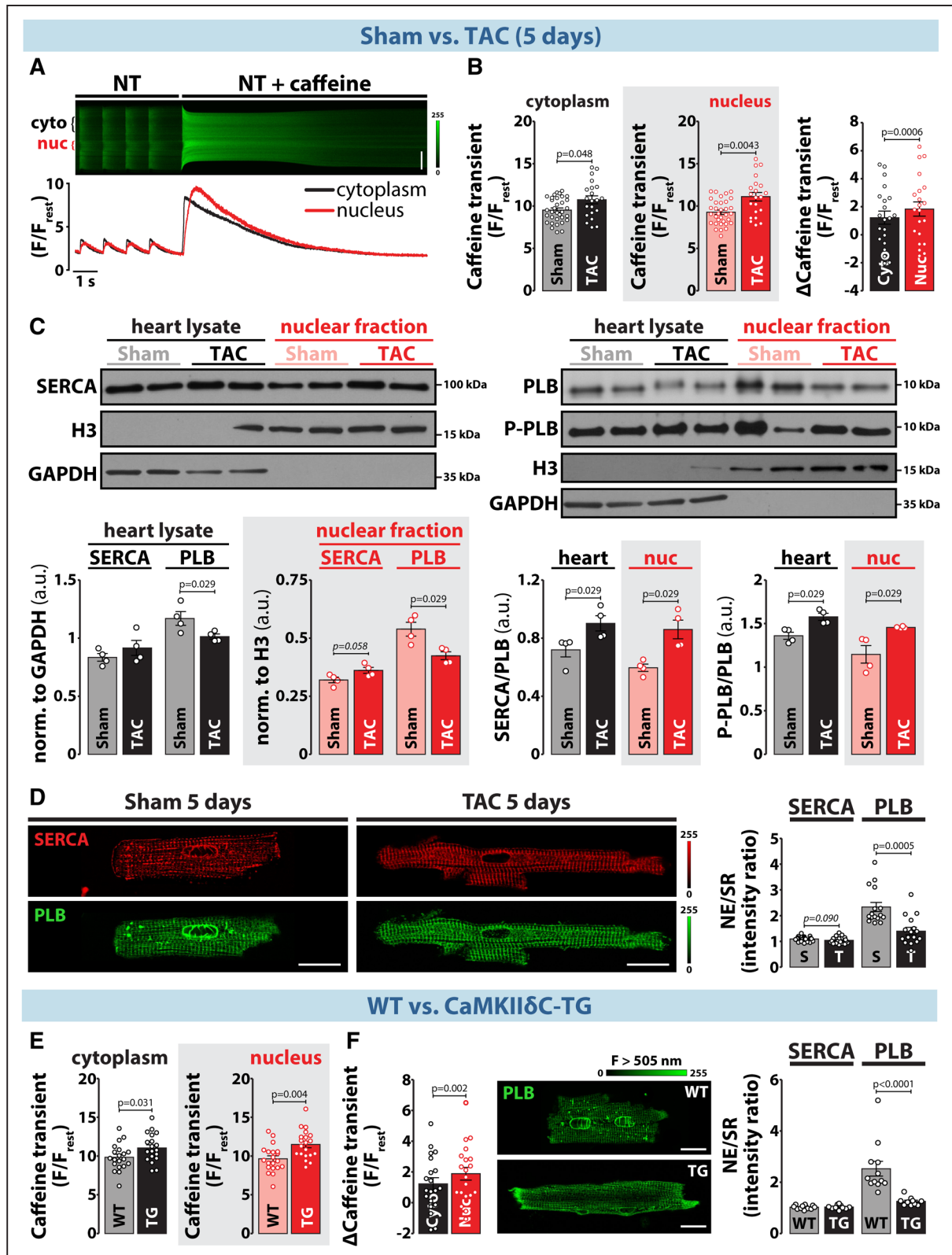
Figure 3. Sarcoplasmic reticulum (SR) and perinuclear Ca²⁺ load and expression and intracellular distribution of major Ca²⁺ reuptake proteins in cardiac hypertrophy due to the pressure overload or CaMKIIδC (Ca²⁺-Calmodulin dependent protein kinase δC) overexpression.

A, Linescan image from a cardiomyocyte from a transaortic constriction (TAC)–operated mouse isolated 5 d after intervention and corresponding normalized nucleoplasmic (nuc, red) and cytoplasmic (cyto, black) fluorescence traces (normalized to resting fluorescence, F/Frest) recorded during caffeine application (**left**). **B**, average values of caffeine-evoked Ca²⁺ transient (CaT) amplitude in cytoplasm and nucleoplasm of ventricular myocytes from sham and TAC-operated mice and increases in SR and perinuclear Ca²⁺ load calculated as difference from sham (ΔF, **right**). n=21–33 myocytes per group. (*Continued*)

elevated SERCA/PLB expression ratios in both compartments (Figure 3C). PLB binds to and decreases SR Ca^{2+}-ATPase activity by lowering its Ca^{2+} sensitivity, so the lower SERCA2/PLB ratio is consistent with faster SR Ca^{2+} uptake rates inferred by faster rates of twitch $[Ca^{2+}]$ decline. Notably, the rise in SERCA/PLB ratio was greater in the nuclear fraction versus heart lysates (300% versus 200%).

Figure 3D shows immunocytochemistry, where we can directly assess SERCA and PLB in the nuclear and cytosolic regions of the myocyte. In sham mice, the PLB signal at the NE was much higher than in the SR (consistent with Wu et al[16]), whereas SERCA levels showed no statistical difference between the 2 loci. During early TAC, PLB appeared to be especially reduced at the NE. This might account, in part, for the relatively strong increase in twitch-associated and caffeine-induced CaTs at the nucleus (Figures 1C and 3A).

Similar results were obtained with young CaMKIIδC-TG mice (Figure 3E and 3F), suggesting that the downregulation of PLB at the NE may be critical in regulating local $[Ca^{2+}]$ in the nuclear region. To the extent that this can modulate nuclear Ca^{2+}-dependent nuclear signaling and transcription, this process may start early in TAC or CaMKIIδC overexpression.

Frequency-Dependent Nucleoplasmic CaTs in Young CaMKIIδC Transgenic Mice

We previously showed that in early TAC higher pacing frequencies elevate diastolic $[Ca]_{Nuc}$ to a much larger extent than diastolic $[Ca]_{Cyto}$, leading to the activation of nuclear CaMKII and HDAC4 nuclear export.[4] Here, we tested for parallel frequency-dependent responses in young CaMKIIδC-TG mice.

Figure 4A shows CaT in 6- to 8-week TG versus WT mice. It is apparent in the images (Figure 1A) and traces (Figure 4B) that as pacing rate increases $[Ca]_{Nuc}$ remains high even during diastole. However, there was little difference in frequency-response of WT and young TG mice (6–8 weeks) regarding either diastolic [Ca], CaT amplitude or decline (for cytosolic and mostly for nucleus; Figure 4C and 4D, Figure IV in the Data Supplement), but data were consistent with the lower diastolic, faster decay and higher CaT amplitudes for young TG versus WT mice as in Figure 2. The most striking difference for early TG mice versus WT was that the CaT

amplitudes were much larger (Figure 4D) and 50% decline much faster (Figure IV in the Data Supplement) in early TG, and the buildup of diastolic $[Ca]_{Nuc}$ was much higher than for $[Ca]_{Cyto}$ at any frequency studied. Notably, in the 6- to 8-week TG mice, time-averaged $[Ca]_{Nuc}$ (ie, the CaT integral/time) was not statistically different from WT at 0.5 Hz but was much higher (≈30%) for any higher frequency studied (Figure 4E). These differences were more modest for $[Ca]_{Cyto}$ in young TG versus WT. This would be consistent with the higher perinuclear SERCA function in early TG (or TAC) mice from Figure 3, which could promote enhanced nuclear Ca^{2+} signaling to CaMKII and HDAC4. Older TG mice (11−13 weeks) show an exacerbated rise in the time-averaged $[Ca]_{Nuc}$, especially at higher pacing rates.

CaMKIIδ Activation and (Peri)Nuclear Accumulation in Young CaMKIIδC-TG Mice

The data presented so far clearly indicate enhancement of nuclear Ca^{2+} signaling and alterations in Ca^{2+} cycling in early pressure overload−induced hypertrophy and young CaMKIIδC-TG mice. We speculate that this suffices to promote Ca^{2+}-dependent hypertrophic gene transcription machinery. Thus, we first sought to assess local CaMKIIδ activation under conditions where we studied $[Ca]_{Cyto}$ and $[Ca]_{Nuc}$ above. We used antibodies against CaMKIIδ and P-CaMKII (phospho-CaMKIIδ) to assess autonomously active CaMKII. Antibody specificity was validated in detail (Figure V in the Data Supplement).

There was little autonomous P-CaMKII evident in sham myocytes at rest, and weak staining at low pacing frequency (0.5 Hz) that increased in both cytosol and nucleus at higher stimulation frequency (5 Hz) particularly at the NE (Figure 5A through 5C). That is reminiscent of the rise in $[Ca]_{Nuc}$ and $[Ca]_{Cyto}$ with pacing (Figure 4) and data using FRET (fluorescence resonance energy transfer)-based CaMKII activity reporters.[17] Early post-TAC (5 days) myocytes showed greater CaMKIIδ activation than sham already at 0.5 Hz; however, we found a clear enhancement of P-CaMKII signal on the SR (cytoplasm) and NE only (Figure 5B). At higher pacing frequency—in contrast to sham hearts—early WT-TAC hearts displayed an excessive CaMKII nuclear import, which resembled that measured 45 days after TAC (but was also present at 0.5 Hz in late TAC). In both TAC groups, P-CaMKII signal escalated dramatically around the NE (ie, even higher than

---

Figure 3 Continued. Scale bar=20 µm. **C**, Western blots (**top**) and average data (**bottom**) of SERCA (SR-Ca^{2+}-ATPase), PLB (phospholamban), and P-PLB (PLB phosphorylated at Thr17) expression in tissue lysates and isolated cardiomyocyte nuclei from LV tissue of sham and TAC-operated mice. GAPDH was used as loading control for tissue lysate samples and H3 as loading control for nuclei samples. N=4 samples per group. **D**, Dual-staining confocal microscopy images with the monoclonal anti-SERCA antibody conjugated with Alexa fluor-594 (**top left**) and monoclonal anti-PLB antibody conjugated with Alexa fluor-488 (**bottom left**) and nuclear envelope (NE)-to-sarcoplasmic reticulum intensity ratio profiles (**right**) in cardiomyocytes from Sham vs TAC-operated mice isolated 5 d after intervention. n=16−20 myocytes per group. Scale bars=20 µm. **E**, Corresponding analyses of caffeine-evoked CaTs and (**F**) subcellular expression of PLB in CaMKIIδC transgenic mice (TG). n=10−20 myocytes per group. *P* values were calculated using Mann-Whitney test comparing TAC or TG to the respective control (**B**−**E**), or Wilcoxon signed-rank test for paired nuclear vs cytoplasmic comparisons (**B** [**right**], **E** [**right**]). Scale bars=20 µm. H3 indicates histone H3; and WT, wild type.
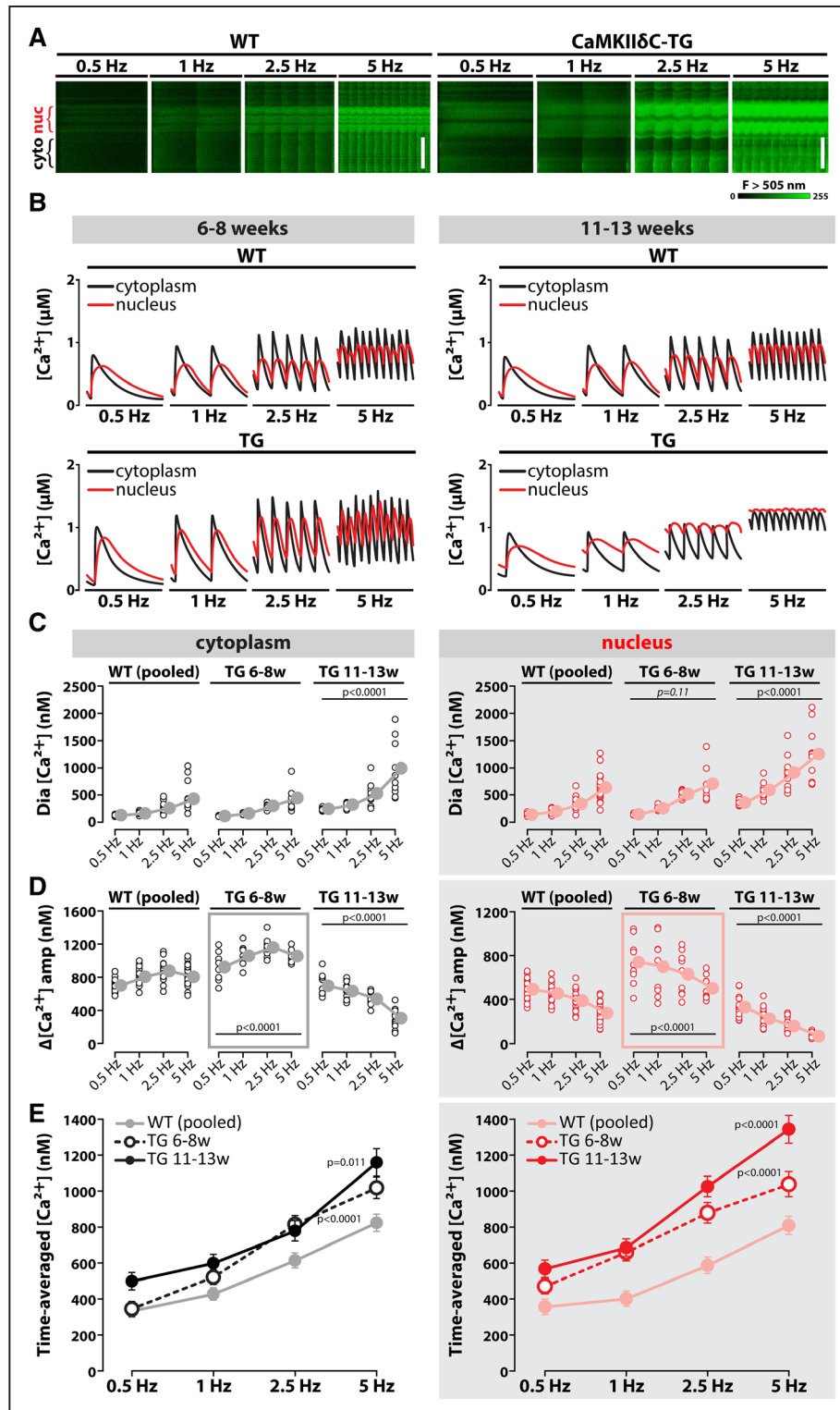
Figure 4. Frequency-dependent changes of nucleoplasmic vs cytoplasmic [Ca²⁺] transients (CaTs) in ventricular mouse myocytes induced by transgenic overexpression of CaMKIIδC (Ca²⁺-Calmodulin dependent protein kinase δC).
A, Linescan confocal images of cytoplasmic (cyto) and nucleoplasmic (nuc) CaTs in a ventricular myocyte isolated at 7 wk of age from wild-type (WT; **left**) and TG (**right**) mouse. Note that the area of higher fluorescence corresponds to nuclear signal (nuc). Scale bar=15 μm. **B**, Averaged original recordings of electrically stimulated CaTs in the nucleus (red) vs cytoplasm (black) of ventricular myocytes isolated from 6 to 8 (**left**) or 11 to 13 (**right**) wk old WT (**top**) and TG (**bottom**) mice during gradual increase of stimulation frequency from 0.5 to 5 Hz. Frequency-dependent changes in (**C**) diastolic [Ca²⁺] and (**D**) amplitude of electrically stimulated CaTs in the cytoplasm (gray) vs nucleus (red) of ventricular myocytes isolated from WT (**left**) and 6–8 (**middle**) or 11–13 (**right**) wk old TG mice. **E**, Time-averaged [Ca²⁺] calculated as time-integral area under CaT-time curve over one cycle of cardiomyocytes isolated from WT and 6–8-wk or 11–13-wk old TG mice. **C–E**, n=8–21 myocytes per group. P values were calculated using Dunnett post hoc test (vs WT control), following significant 2-way repeated-measures ANOVA.
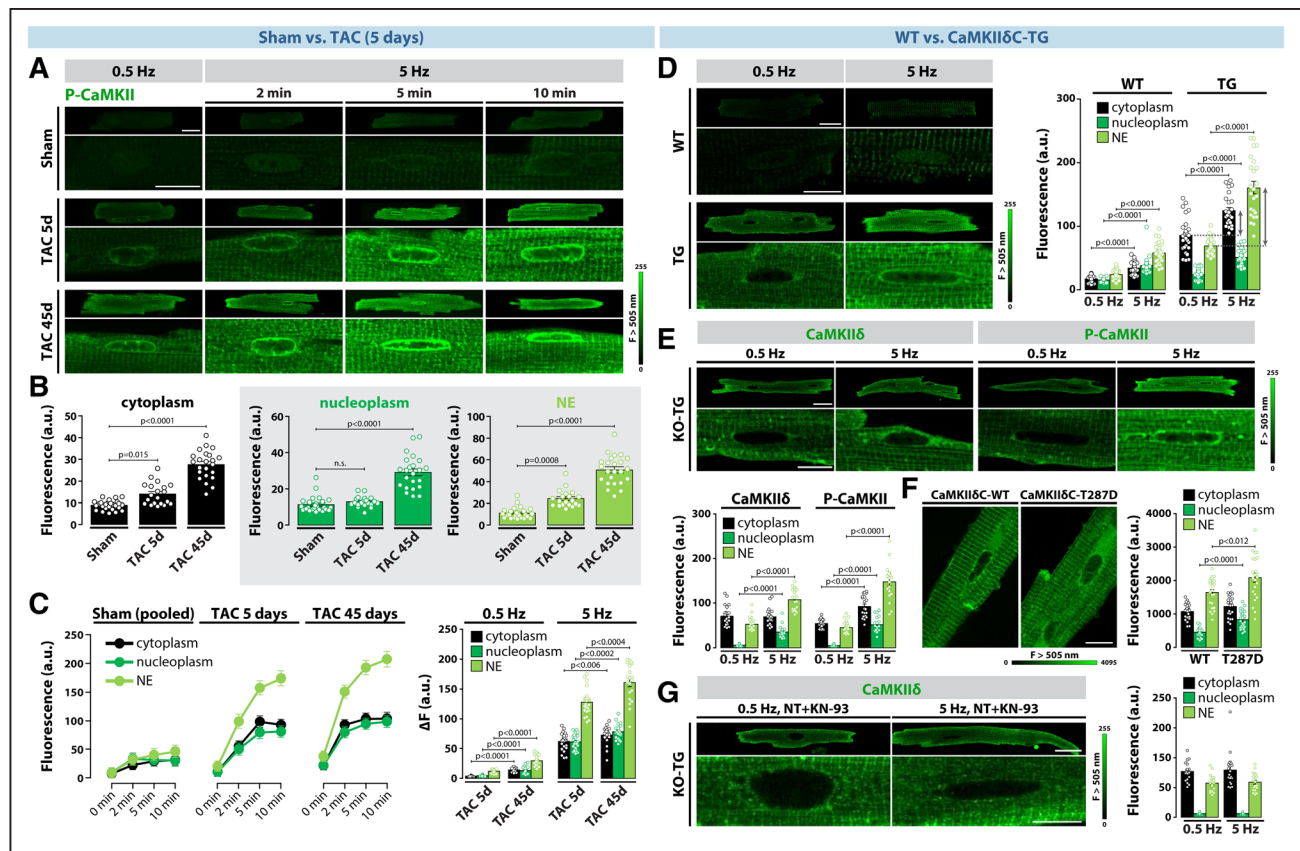
Figure 5. High-pacing frequency-dependent CaMKIIδ (Ca²⁺-Calmodulin dependent protein kinase δ) phosphorylation and its subcellular redistribution in cardiac hypertrophy due to the pressure overload or CaMKIIδC overexpression.
A, Original confocal images of cardiomyocytes from sham-operated (**top**) and transaortic constriction (TAC)–operated mice (5 and 45 d after intervention, **middle** and **bottom**, respectively) immunostained for P-CaMKII (phospho-CaMKII) after stimulation at 0.5 (**left**) or 2, 5, and 10 min of stimulation at 5 (**right**) Hz. **B**, Average P-CaMKII fluorescence values (arbitrary units, a.u.) in cytoplasm (black), nucleoplasm (dark green), and nuclear envelope (NE, light green) of cardiomyocytes from sham-operated and TAC-operated mice isolated 5 and 45 d after intervention, stimulated at 0.5 Hz. **C**, Average P-CaMKII fluorescence values (**left**) in time-dependent high-pacing protocol and increases in P-CaMKII levels calculated as difference from sham (ΔF, **right**) in cytoplasm (black), nucleoplasm (dark green), and nuclear envelope (NE, light green) of cardiomyocytes from sham-operated and TAC-operated mice isolated 5 and 45 d after intervention. **D**, Corresponding analyses of CaMKII phosphorylation and redistribution in 6–8-wk old CaMKIIδC transgenic mice (TG). **E**, Original confocal images of cardiomyocytes from 6- to 8-wk old CaMKIIδ knockout mice with transgenic overexpression of CaMKIIδC (KO [CaMKIIδ-knockout]-TG) immunostained for CaMKIIδ (**top left**) and P-CaMKII (**top right**) after 5 min stimulation at 0.5 or 5 Hz and corresponding average CaMKIIδ (**bottom left**) and P-CaMKII (**bottom right**) fluorescence values in cytoplasm (black), nucleoplasm (dark green) and nuclear envelope (NE, light green). **F**, Original confocal images of isolated ventricular rabbit myocytes expressing GFP (green fluorescent protein)-labeled wild-type (WT) CaMKIIδC (WT; **left**) vs its autophosphorylation-mimetic T287D-δC-GFP (T287D, **right**) and corresponding average fluorescence values in cytoplasm (black), nucleoplasm (dark green) and NE (light green). **G**, Original confocal images of cardiomyocytes from 6- to 8-wk old CaMKIIδ knockout mice with transgenic overexpression of CaMKIIδC (KO-TG) preincubated with N-[2-[[[(E)-3-(4-chlorophenyl)prop-2-enyl]-methylamino]methyl]phenyl]-N-(2-hydroxyethyl)-4-methoxybenzenesulfonamide (KN-93) and immunostained for P-CaMKII after 5 min stimulation at 0.5 or 5 Hz (**left**) and corresponding average P-CaMKII (**right**) fluorescence values in cytoplasm (black), nucleoplasm (dark green) and NE (light green). **B–G**, n=20–30 myocytes per group. *P* values were calculated using Kruskal-Wallis with Dunn post hoc test (**B**) or Mann-Whitney test comparing 45 d, 5 Hz, or T287D to the respective control (**C–G**). Scale bars=20 μm for the whole cell and 10 μm for the zoomed nucleus. NT indicates normal tyrode.

inside the nucleus) upon pacing at 5 Hz. This raises the possibility that early on in TAC, active CaMKIIδ accumulates in the perinuclear region, where it can preferentially phosphorylate local targets. For example, nuclear CaMKII can phosphorylate HDAC4, driving nuclear export, but a pool of active perinuclear CaMKII may promote rephosphorylation of any exported HDAC4 that happens to get dephosphorylated after leaving the nucleus. That could help keep dephosphorylated HDAC4 from reentering the nucleus and reinforce the transcriptional effects of

CaMKII activation. Indeed, our previous studies proved the role of non-nuclear CaMKIIδ in maintaining HDAC4 in the cytosol.[18] The P-CaMKII signals above were prevented by KN-93 preincubation (Figure 1G), confirming the functional role of CaMKII activity in the observed signals.

Figure 5D shows analogous results in young CaMKIIδC-TG mice (6–8 weeks), suggesting that the CaMKIIδC variant suffices to produce this strong perinuclear CaMKII activation. One difference versus TAC was that young TG mice showed substantial phosphorylation

of cytosolic CaMKII even at low frequency (black bars in Figure 5D versus 5B), which may be in part due to the higher absolute levels of CaMKIIδ present in the TG myocytes versus TAC-induced upregulation of CaMKIIδ expression (Figure III in the Data Supplement).

To further test whether CaMKIIδC alone, in the absence of CaMKIIδB, can cause robust perinuclear accumulation of active CaMKII, we examined KO-δCTG. Figure 5E shows that 5-minute pacing at 5 Hz in these KO-δCTG myocytes caused prominent perinuclear CaMKIIδC and P-CaMKIIδC accumulation, which was prevented by preincubation with KN-93 (Figure 5G). Thus CaMKIIδC does not rely on CaMKIIδB to promote the pacing-induced nuclear and perinuclear CaMKII activation.

Finally, we overexpressed GFP (green fluorescent protein)–tagged WT CaMKIIδC and a P-CaMKII– mimetic CaMKIIδC-T287D mutant. Notably, the auto-phosphorylation-mutant was more nuclear (1.5-fold in the nucleoplasm and 1.2-fold on the NE), suggesting that CaMKIIδC activation indeed directs its nuclear localization (Figure 5F).

Pacing-Dependent Nuclear HDAC4 Export in Young CaMKIIδC Transgenic Mice

The higher levels of nuclear and perinuclear active CaMKII would be expected to promote HDAC4 nuclear export. Figure 6A shows HDAC4 localization in quiescent young (6–8 weeks) WT, CaMKIIδC-TG, CaMKIIδ-KO, and KO-δCTG mice. At baseline, the CaMKIIδC-KO versus WT exhibits higher nuclear HDAC4 compared with cytosolic and perinuclear levels (F_{Nuc}/F_{Cyto} and F_{Nuc}/F_{PN}; Figure 6B), consistent with the KO preventing a baseline level of CaMKIIδ-dependent HDAC4 nuclear export. Conversely, CaMKIIδC overexpression without CaMKIIδB (KO-δCTG) reduced baseline nuclear HDAC4, expressed relative to either cytosolic or perinuclear, compared to WT (Figure 6B). So CaMKIIδC by itself can drive nuclear export of HDAC4. Straight CaMKIIδC-TG mice (which also have CaMKIIδB) showed higher F_{Nuc}/F_{PN} but not F_{Nuc}/F_{Cyto}. Conceivably, CaMKIIδB limits the baseline effect of CaMKIIδC on HDAC4, as has been suggested with respect to ischemia/reperfusion damage.[8]

High-pacing frequency drove time-dependent HDAC4 nuclear export in WT mice, which was accelerated in TG mice, and prevented in KO mice (Figure 6C through 6E). Of note, there is a temporary retention of exported HDAC4 in the perinuclear region, evidenced by an increase in F_{PN}/F_{Cyto} peaking at ≈10 min in TG, which was smaller and later in WT (Figure 6F). Although the F_{Nuc}/F_{Cyto} declined continuously throughout the pacing protocol and reached similar values in WT and TG mice at 25 to 30 minutes (Figure 6E and 6F), the perinuclear retention of HDAC4 was prominent earlier but also dissipated faster in TG mice. This could result

from the faster rate of HDAC4 export in TG and then consequently faster diffusion away from the perinuclear region. Faster movement of HDAC4 further throughout the cytosol could also slow the reversal of pacing (or GPCR [G-protein–coupled receptor] activation) induced HDAC4 nuclear derepression. To test this, we monitored the recovery of F_{Nuc}/F_{Cyto} upon reduction of pacing from 5 to 0.5 Hz at 15 minutes (Figure 6G). There was much faster recovery of nuclear HDAC4 in the WT than TG within 15 minutes (70 versus 20%). Thus, short-term accumulation of HDAC4 in the perinuclear region can allow faster reversal of transcriptional effects that are controlled by HDAC4 nuclear export.

To confirm our observations regarding HDAC4 translocation in real-time live-cell imaging, we used ventricular myocytes in which GFP-tagged HDAC4 was expressed via adenovirus (Figure 6H through 6J). Pacing here was at only 1.5 Hz (due to use of cultured myocytes), and that may explain the slower overall nuclear HDAC4 export; however, we still detected significant perinuclear accumulation at this pacing rate (Figure 6H). Our related work demonstrating nuclear $InsP_3R$ and CaMKII involvement in GPCR-triggered HDAC5 nuclear export did not detect nuclear export in rabbit ventricular myocytes in response to 0.5 to 1 Hz stimulation.[19] Thus, rapid nuclear HDAC export that is driven solely by CaTs may require high-pacing rates (as implicit in Figure 6G).

These findings are in agreement with our subcellular Ca^{2+} and HDAC4 data upon pressure overload. Namely, in the early TAC at baseline CaMKIIδC appears to be involved in enhancement of cytoplasmic and particularly nucleoplasmic CaTs (Figure 1), without changes in HDAC4 localization (Figure VI in the Data Supplement). In late TAC, CaMKIIδC is already accumulated in the nucleus and has a prominent role in ETC, as evidenced by reduced levels of nuclear HDAC4 at baseline (Figure VI in the Data Supplement). Collectively, our data suggest that CaMKIIδC might play a dual role in the early phase after TAC; (1) CaMKIIδC primarily regulates the ECC, and, thus, promotes survival under baseline conditions (Figure 1A through 1I and Figure VII in the Data Supplement), whereas (2) under stress, it translocates to the nucleus (Figure 5) and stimulates the ETC (Figure 6).

CaMKII Activation Versus Nuclear Translocation Determines Myocytes Genetic Profile

To further test whether the intensity of nuclear CaMKII activation differentially modulates pathological gene expression profiles, we used neonatal rat ventricular cardiomyocytes with pacing protocols that we found to induce similar increases in time-averaged $[Ca^{2+}]_i$ as in early TAC mice or 6- to 8-week old CaMKIIδC-TG mice at high-pacing rates in Figure 4E. Neonatal rat ventricular cardiomyocytes stimulated at 8 Hz for 3 hours produced modest overall CaMKII activation, but not nuclear
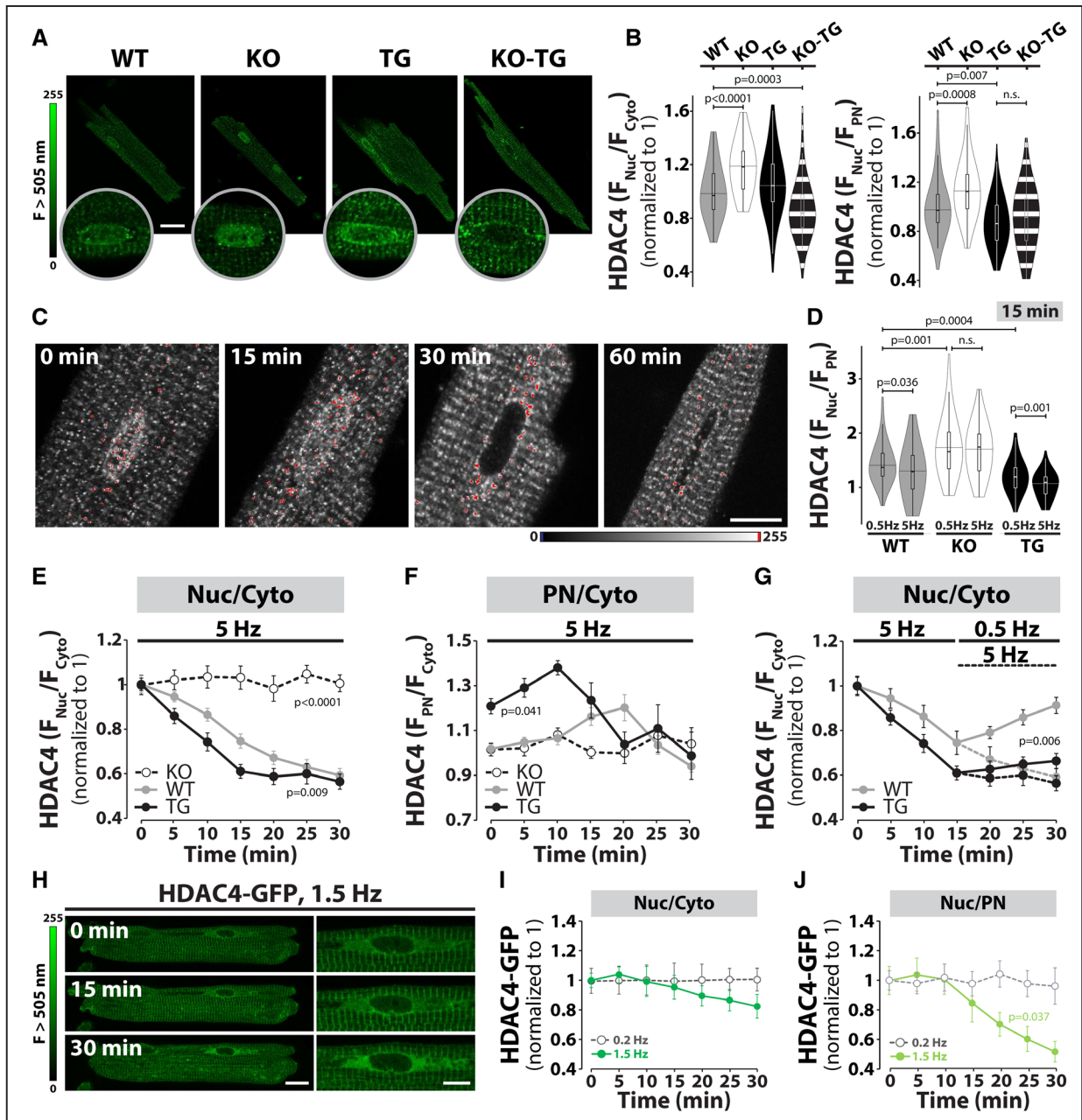
Figure 6. HDAC4 (histone deacetylase) redistribution and high-pacing frequency-dependent translocation in electrically stimulated ventricular myocytes isolated from 6- to 8-wk old CaMKIIδ-KO (Ca²⁺-Calmodulin dependent protein kinase δ knockout), wild-type (WT) and mice with transgenic overexpression of CaMKIIδC in WT or KO background.

A, Original confocal images of cardiomyocytes from 6- to 8-wk old CaMKIIδ-KO (KO), WT, and mice with transgenic overexpression of CaMKIIδC in WT (TG) or KO (KO-TG) background immunostained for HDAC4. **B**, Corresponding subcellular distribution calculated as nucleo-to-cytoplasmic (**left**) or nucleo-to-perinuclear region (PN, **right**) fluorescence ratio (F_{Nuc}/F_{Cyto} and F_{Nuc}/F_{PN}). Scale bar=20 μm. **C**, Representative images of HDAC4 nu ($F_{Nuc}/F^{Cyto \text{ and } F}Nuc/F_{PN}$) clear translocation in response to high-frequency stimulation (5 Hz) in cardiomyocytes isolated from 6- to 8-wk old TG mouse hearts, detected by immunostaining. Scale bar=10 μm. Contrast is enhanced to 1% saturation for better visualization of HDAC4-rich regions. **D**, HDAC4 redistribution in response to high-pacing frequency (5 Hz, 15 min) in cardiomyocytes isolated from WT, KO, and TG mice at 6–8 wk of age. **B**–**D**, n=70–80 myocytes per group. Pacing-induced time-dependent HDAC4 nuclear export calculated as (**E**) nucleo-to-cytoplasm or (**F**) PN-to-cytoplasm region fluorescence ratio in ventricular myocytes isolated from 6- to 8-wk old CaMKIIδ-KO (KO, white), WT (gray) and CaMKIIδC-TG (TG, black) mice. **G**, HDAC4 nuclear reentry after cessation of high pacing calculated as nucleo-to-cytoplasm fluorescence ratio in ventricular myocytes isolated from 6- to 8-wk old CaMKIIδ-KO (KO, white), WT (gray), and CaMKIIδC-TG (TG, black) mice. n=9–17 myocytes per group. **H**, Representative confocal images of cultured adult cardiomyocyte infected with HDAC4-GFP (green fluorescent protein), paced at 1.5 Hz for 0, 15, or 30 min. Scale bars=20 μm for the whole cell and 10 μm for the zoomed nucleus. Time course of HDAC4 translocation is measured as (**I**) (I) nucleo-to-cytoplasmic (Nuc/Cyto) or (**J**) nucleo-to-perinuclear fluorescence ratios in response to low (gray) or high (green) pacing frequency. n=8–10 cells per group. *P* values were calculated using Kruskal-Wallis with Dunn post hoc test (**B**, and genotypes in D), Mann-Whitney test comparing 5 Hz and 0.5 Hz (**D**), or 2-way ANOVA (**E–G**) that was repeated measures in (**I–J**) and adjusted by Dunnett post hoc (vs WT) in case of multiple comparisons (**E–F**).

CaMKII accumulation (Figure VIIA through VIIC in the Data Supplement). An intriguing aspect of these results is that CaMKII inhibition with KN-93 at the early TAC/TG mimicking condition (8 Hz) promoted the largest myocyte hypertrophy and expression of *NppB* and interleukin-6 receptor (*IL6R*). This hints that perhaps CaMKII activation in this condition is positively adaptive[11] perhaps because of the enhanced SR Ca^{2+} uptake that prevents nuclear Ca^{2+} overload (Figures 1 through 3), at least for brain natriuretic peptide (BNP) and IL6R expression.

Pushing $[Ca^{2+}]_i$ further by raising $[Ca^{2+}]_o$ to 3 mmol/L (mimicking more the 11-–13-week TG) resulted in robust enhancement of nuclear CaMKII and increased myocyte size (Figure VIID in the Data Supplement). This was also accompanied by transcriptional upregulation of well-established marker genes linked to pathological hypertrophy: *NppB* (BNP), *RCAN-1, IL6R,* and transforming growth factor (*TGF*)-*β1* (Figure VIIE in the Data Supplement). Notably, the *RCAN-1* and *TGF-β1* upregulation was prevented by CaMKII inhibitor KN-93, underscoring the important role of nuclear CaMKII activation in this pathological progression.[11] Indeed, TGF-β has been reported to have a prominent role in advanced stage of pressure overload, and its suppression in cardiomyocytes is protective against maladaptive cardiac remodeling.[20,21]

Increased CaMKIIδC Activation, and (Peri) Nuclear Accumulation Promotes Eccentric Cardiac Hypertrophy

We next analyzed structural changes seen during the progressive hypertrophy in WT, KO, and transgenic mice overexpressing CaMKIIδC in WT (TG) or the CaMKIIδ null background (KO-δCTG). CaMKIIδ KO mice showed no statistical difference to WT in nearly all parameters measured in Figure 7 (including heart weight, lung weight, myocyte, and nucleus dimensions) for both young and older mice. The only difference was a minor reduction in cell width in the KO versus WT mice in young animals.

High levels of CaMKIIδC found in both CaMKIIδC-TG and KO-δCTG mouse lines (around 7-fold increase over endogenous CaMKII, Figure IIIA in the Data Supplement) could induce nonspecific cellular distributions and unspecific kinase effects. Our previous work confirmed that overexpressed CaMKIIδC was similarly distributed among cytosolic, mitochondrial, SR, and nuclear fractions as for endogenous CaMKIIδC, even when CaMKIIδC was expressed in the KO background.[6] In addition, at the sarcomeric level, both endogenous and overexpressed CaMKIIδ are highly concentrated at the Z-line, with additional midsarcomere and nuclear signal.[7] This is consistent with the well-documented association of CaMKII with RyR2 located at the SR. This sarcomeric profile of CaMKIIδ was seen in our immunofluorescent images of WT, TG, and KO-δCTG ventricular myocytes (Figure IIIC in the Data Supplement). Also, perinuclear

CaMKII at baseline in WT mice was uniform throughout the nucleus, TG mice had comparable level intranuclear, but higher at the NE, whereas KO-δCTG mice showed low nucleoplasmic signal (due to the loss of CaMKIIδB) and prominent NE signal, as in TG mice. Most importantly, transgenically overexpressed CaMKIIδC behaves functionally much like the TAC-induced overexpressed CaMKIIδC with respect to nuclear translocation that also drives hypertrophy.

Both CaMKIIδC transgenic mice, CaMKIIδC-TG and KO-δCTG, showed cardiac hypertrophy resulting in the development of HF (Figure 7A and 7B). Although the extents of CaMKIIδC overexpression was not statistically different (Figure III in the Data Supplement), KO-δCTG mice showed remarkably accelerated remodeling and transition to HF compared to TG mice, as evidenced by a larger and earlier increases in heart weight-to-body weight ratio and signs of pulmonary edema (Figure 7A and 7B). In addition, KO-δCTG cardiomyocytes showed exclusively eccentric growth, with a large increase in cell length but unaltered cell width over time (Figure 7C and 7D). TG myocytes exhibited balanced concentric-eccentric growth, such that myocyte length/width ratio was unaltered at 6 to 8 weeks and only minimally increased at weeks 11 to 13 (compared with WT). Different modes of myocyte growth resulted in an increase in ventricular wall thickness without chamber enlargement in young TG mice (concentric hypertrophy),[13] whereas cell lengthening promoted chamber dilatation with severely depressed cardiac function, already in 6- to 8-week old KO-δCTG mice.[8] KO-δCTG mice also showed high early mortality and shorter lifespan compared with TG mice, and with aging, these mice exhibited extreme dilatory growth. Figure 7E and 7F shows that nuclear growth followed similar pattern of length-width ratios as the myocyte growth, and could relate to a role for changed NE structure in promoting cardiac pathology.[4]

CaMKIIδC Activation and (Peri)Nuclear Accumulation Is a Hallmark of HF

We had access to nonfailing and failing human myocardium to perform comparative analyses of CaMKIIδ expression in TAC mice and in human HF tissue and nuclear fractions (Figure 8). The enrichment of selected fractions was confirmed by using additional markers of cellular compartments (eg, Na^+/K^+-ATPase for plasma membrane and Nup62 for nuclear membrane) and confocal imaging of purified nuclear fraction (Figure VIII in the Data Supplement). Western blots with left ventricular tissue lysates (Figure 8A and 8B and 8E and 8F) and isolated cardiomyocyte nuclei (Figure 8C and 8D and 8G and 8H) revealed a large increase of CaMKIIδ expression in both tissue and isolated nuclear fractions in failing versus nonfailing hearts. The large increase in nuclear expression of CaMKIIδ in failing hearts appeared
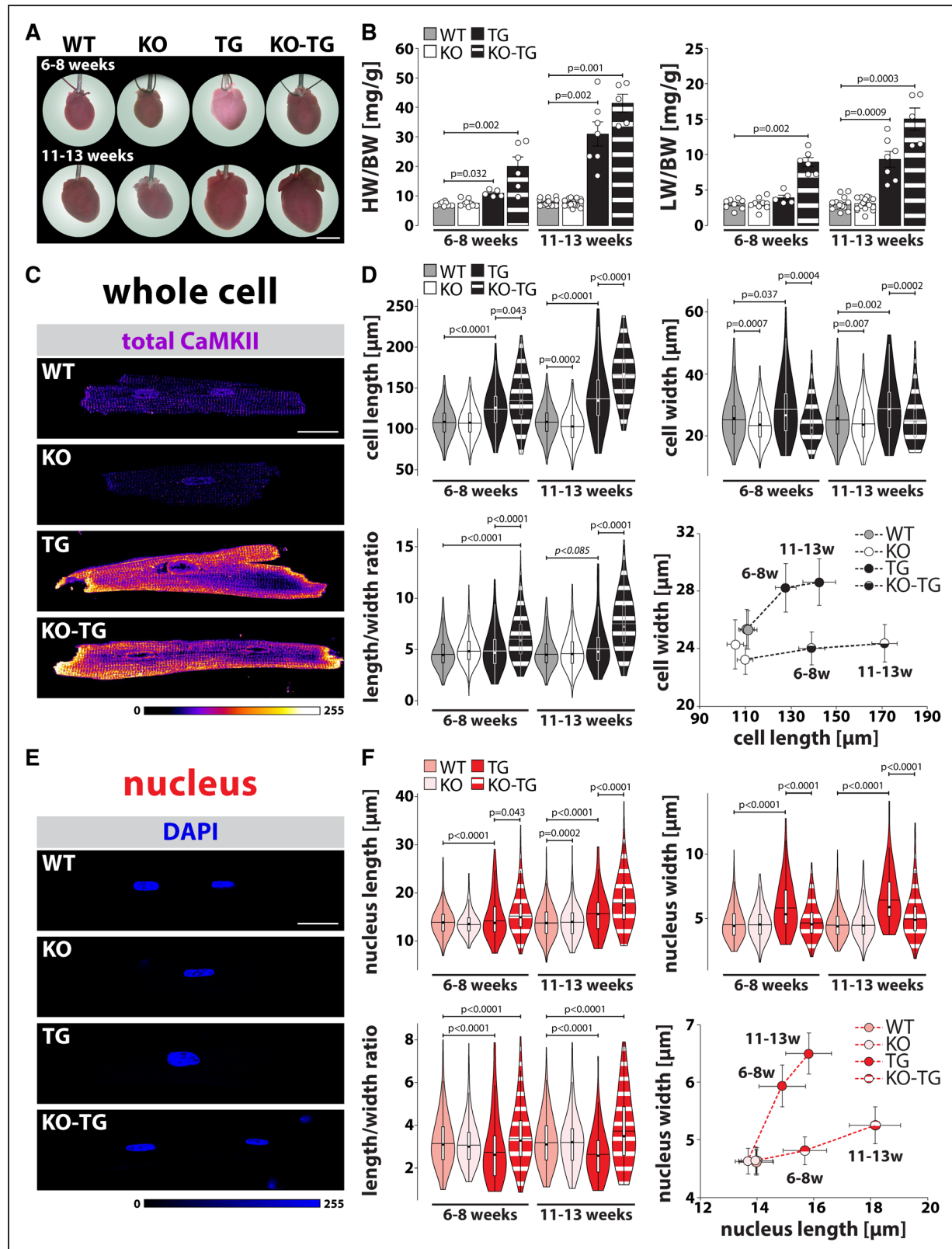
Figure 7. Characterization of hypertrophic growth of the heart, cardiomyocytes, and nuclei in 6–8-wk and 11–13-wk old CaMKIIδ-KO (Ca²⁺-Calmodulin dependent protein kinase δ knockout), wild-type (WT) and mice with transgenic overexpression of CaMKIIδC in WT or KO background.

A, Photomicrographs of hearts taken at age 6–8 wk (**top**) and 11–13 wk (**bottom**). Scale bar is 5 mm. **B**, Heart weight or lung weight normalized to body weight. N=5–18 per group. **C**, Original 2-dimensional (2D) images of cardiomyocytes isolated from CaMKIIδ-KO (KO), WT, and mice with transgenic overexpression of CaMKIIδC in WT (TG) or KO (KO-TG) background at 11–13 wk following (*Continued*)

to be due to the accumulation of CaMKIIδC isoform in the nuclear region (Figure 8C and 8D and 8G and 8H), underscoring the pivotal role of increased CaMKIIδC activation and (peri)nuclear accumulation in eccentric cardiac hypertrophy, both in mouse model and in failing human hearts.

DISCUSSION

Although CaMKIIδ has emerged as a promising target in cardiac remodeling over the past 2 decades,[22–25] more nuanced understanding of its splice variants and activation state regulation is required for more precision targeting.[6,26,27] Here, we provide compelling evidence for the critical role of CaMKIIδC activation, secondary to very early enhancement of cytoplasmic and especially nucleoplasmic Ca^{2+} signaling in a mouse model of pressure overload and in failing human hearts. This enhanced Ca^{2+} signaling further promotes CaMKIIδC activation, leading to its (peri)nuclear accumulation and promotion of eccentric cardiac growth. The autoreinforcing property of CaMKIIδC signaling, via interplay between ECC and ETC, is critical for the progression of cardiac hypertrophy to HF.[28]

Remarkable Parallelism in Early TAC and Early CaMKIIδC Transgenic Mice

CaMKIIδC expression is selectively increased as early as one day post-TAC.[13,29] What struck us here was the remarkable parallelism of changes observed in early TAC (5 days) and early CaMKIIδC-TG mice (6 to 8 weeks) before any overt pathological effects. Indeed, at this stage in both groups the CaT amplitude, rate of $[Ca^{2+}]_i$ decline and SR Ca^{2+} content were all increased, especially at the nucleus. Additionally, PLB phosphorylation was increased, its expression was reduced, especially near the nucleus, in both models (in line with enhanced SERCA function as observed here as faster twitch $[Ca^{2+}]_i$ decline). Early CaMKIIδ TG mice also exhibited nuclear remodeling as did 1-week post-TAC in our prior study.[4] CaMKII was also more concentrated in the nuclear/perinuclear region and more activated in both models, and both early models already showed increased HDAC4 nuclear export. The fact that early CaMKIIδC overexpression can recapitulate the same tableau of effects as early TAC (including the CaMKII activation) raises the possibility that TAC-induced CaMKII activation may be an early compensatory response that boosts myocyte CaTs and contractility to meet the imposed afterload.

Indeed, we show that the extent of nuclear CaMKII activation correlates with activation of gene expression of selected well-known remodeling marker genes in neonatal rat ventricular cardiomyocytes. This was most clear for *RCAN-1* and *TGF-β1*, where KN-93 also prevented the Ca-dependent effects. However, for *NppB* and *IL6R*, CaMKII inhibition exacerbated the rise in gene expression, suggesting increased complexity. One possibility is that the beneficial side of CaMKII activation seen in early TAC and CaMKIIδC-TG might also restrain somehow the induction of *NppB* and *IL6R*.

As both TAC and CaMKIIδC-TG mice age further they progress to major cardiac hypertrophy and transition to HF with lung congestion, greatly reduced ejection fraction and reduced myocyte CaT amplitudes with slowed $[Ca^{2+}]_i$ decline (at 6–7 weeks for TAC and 11–13 weeks in CaMKIIδ TG). Notably, as mice in both of these models develop HF, the time-averaged nuclear $[Ca^{2+}]$ and (peri)nuclear CaMKII level and activity is further enhanced which may reinforce the nuclear CaMKII and HDAC4 signaling and their sequelae. This chronic CaMKII activation in the HF stage may no longer be compensatory but may progress to being maladaptive, as indicated by prominent CaMKIIδ- and RyR-dependent SR Ca^{2+} leak that can be proarrhythmic and reduce SR Ca^{2+} content.[12,30] Chronic CaMKIIδ activation in HF can alter the function of many ion channels in ways that worsen function and promote arrhythmias.[5,31] Indeed, CaMKIIδ-KO mice are particularly protected in the transition from compensated hypertrophy to overt HF, and this includes a dramatic limitation in the development of cardiac fibrosis.[21,28]

Enhanced SR and NE Ca^{2+} Stores in Early TAC and CaMKIIδ TG Mice

The amplitude of caffeine-evoked cytoplasmic and nucleoplasmic CaTs were both increased in TAC mice, but the relative increase was larger in the nucleus, suggesting differential regulation of NE versus SR Ca^{2+} load in early remodeling. Indeed, although SERCA2 expression was unchanged in either nuclear or cytoplasmic compartment, PLB expression was decreased in both subcellular spaces, and most dramatically in the nuclear compartment. Consequently, the SERCA/PLB ratio was most evidently increased in the nuclear fraction. Wu et al[16] recently showed that PLB is especially concentrated at the NE, and our myocyte immunostaining and fractionation studies confirm that (Figure 3). However, following TAC or upon transgenic CaMKIIδC overexpression the PLB levels around the nucleus dropped markedly, largely

---

Figure 7 Continued. immunostaining for total-CaMKII. Scale bar=20 µm. **D**, Cardiomyocyte dimensions (**top**), cell length-to-width ratio, and cell length in conjunction with cell width (**bottom**). n=100–500 cells per group. **E**, Original 2D images of cardiomyocytes isolated from CaMKIIδ-KO (KO), WT, and mice with transgenic overexpression of CaMKIIδC in WT (TG) or KO (KO-TG) background at 11–13 wk following DAPI staining for visualization of nuclei. Scale bar=20 µm. **F**, Nucleus dimensions (**top**), nucleus length-to-width ratio, and nucleus length in conjunction with nucleus width (**bottom**). n=100–500 nuclei per group. Indicated. *P* values were calculated using Kruskal-Wallis with Dunn post hoc test. BW indicates body weight; DAPI, 4′,6-diamidino-2-phenylindole; HW, heart weight; and LW, lung weight.
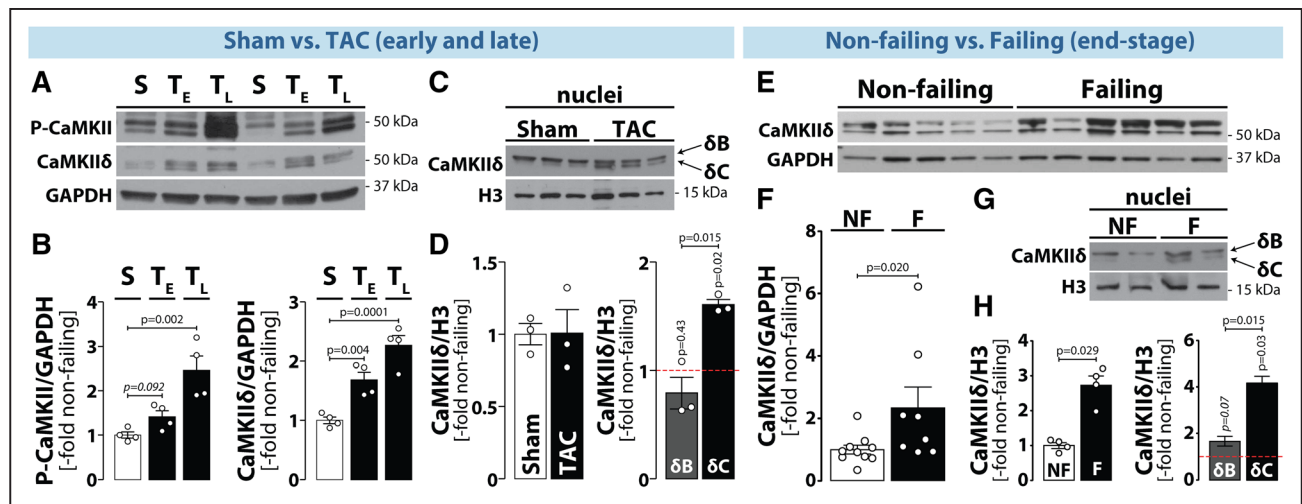
Figure 8. Expression of CaMKIIδ (Ca²⁺-Calmodulin dependent protein kinase δ) in tissue lysates vs isolated cardiomyocyte nuclei from nonfailing and failing human hearts.

A, Western blots and (**B**) average data of CaMKIIδ and P-CaMKII (phospho-CaMKII) expression in tissue lysates from sham (S) and early (5–7 d, T_E) and late (3–6 wk, T_L) transaortic constriction (TAC)–operated mice. **C**, Western blots and (**D**) average data of CaMKIIδ expression in isolated nuclei from S and T_L TAC-operated mice. **A** and **B**, N=4 mice per group. **C** and **D**, pool of N=6 mice per group in 3 technical replicates, GAPDH and H3 were used as loading control for tissue lysate or nuclei samples, respectively. **E**, Western blots and (**F**) average data of CaMKIIδ expression in tissue lysates and (**G** and **H**) isolated nuclei from nonfailing and failing human hearts. Gapdh and H3 were used as loading control for tissue lysate or nuclei samples, respectively. N=8–10 per group; 4 technical replicates. *P* values were calculated using ANOVA with Dunnett post hoc test (**B**), Mann-Whitney test comparing TAC or F to the respective control, or Wilcoxon signed-rank test for paired δC vs δB comparisons (**D**, **F**, and **H**). F indicates failing human hearts; H3, histone H3; and NF, nonfailing human hearts.

eradicating the apparent NE/SR PLB/SERCA2 ratio. This downregulation of PLB in CaMKIIδC-TG cardiomyocytes was previously reported,[12] but here we show that this is especially true around the nucleus. Although PLB expression is typically reduced and its phosphorylation is enhanced in HF, the mechanism of PLB downregulation is not understood. It has been recently shown that PLB is, at least partially, oligo-ubiquitinated at Lys3 and degraded through phosphorylation-mediated polyubiquitination during HF.[32] As PLB is overproportionally phosphorylated around nucleus, this negative feedback mechanism may well be responsible for preferential decrease in PLB levels around nucleus. The predominant reduction of PLB levels around nucleus may contribute to the higher nuclear/perinuclear $[Ca^{2+}]_i$ levels observed here, which may promote both higher local CaMKII activation as well as higher net HDAC4 phosphorylation by CaMKII, a process known to mediate nuclear export of HDAC4 and derepression of Mef2-dependent transcription.[33]

Perinuclear CaMKII and HDAC4 as a New Local Signaling Microdomain

The perinuclear region (PN) may indeed be a key microdomain for exactly this type of signaling. Our previous work suggested that NE SERCA pumps are mainly on the outer leaflet and that most RyR2 channels are in the nearby SR membrane but largely excluded from the NE,[4] despite the fact that the NE membranes (and lumen) are continuous with that of the SR.[19] This means that normal nuclear CaTs are mainly driven by Ca²⁺ release from near-nuclear RyR and diffusion through nuclear pores,[10] and that $[Ca^{2+}]_{Nuc}$ decline requires diffusion back out of the nucleus to be re-sequestered via NE/SR SERCA2 pumps. The higher Ca²⁺ fluxes through this very region, as suggested by the data presented here, may poise this system for dynamic Ca²⁺ signaling that influences CaM-CaMKII and CaM-calcineurin signaling and translocation across the NE.

The Ca²⁺-related microdomain described above may also encompass the large mAKAP (muscle A-kinase anchoring protein) signaling complex that is localized just outside the NE and includes PKA (protein kinase A) and calcineurin.[34] Together this PN microdomain may tune the signals (and molecules) that get into the nucleus to influence gene transcription and also create a local buffering environment for some of these molecules, keeping them available for import upon demand. This is precisely what we hypothesize for the perinuclear accumulation of HDAC4 that we observed in Figure 6F. That is, the acute HDAC4 nuclear export observed upon CaMKII activation could be sustained by high PN CaMKII activity (to rephosphorylate any exported HDAC4 that happens to get dephosphorylated), thereby maintaining nuclear HDAC4 depletion. Then, once the CaMKII signal is reduced, this local pool of HDAC4 can quickly reenter the nucleus to help turn off the transcriptional switch. Having some of this HDAC4 remain local may speed this turn off compared to what would occur if all the exported

HDAC4 went to the far reaches of the cytosol (as in Figure 6G).

Frequency- and GPCR-Induced Changes in [Ca]$_{Nuc}$ versus [Ca]$_{Cyto}$

Here and elsewhere[4,10] we have highlighted that simply increasing stimulation frequency preferentially promotes nuclear Ca^{2+} accumulation, as a consequence of the slower decline of the nuclear versus cytosolic CaTs, and consequent rising of diastolic and time-averaged [Ca]$_{Nuc}$. That by itself can promote Ca^{2+}-dependent activation of nuclear signaling (eg, via CaMKII, as shown here). However, physiologically higher heart rates are accompanied by β-adrenergic receptor activation which (via PKA effects on Ca^{2+} current and SR Ca^{2+} uptake) further increase the CaT amplitude and perforce drive harder the Ca^{2+}-CaMKII signaling described here. In addition, the relative paucity of PLB at early times of TAC and in CaMKIIδ TG mice would limit the PKA-dependent acceleration of local PN [Ca^{2+}]$_i$ decline. Notably, PKA can also phosphorylate HDAC4/5 and favor their nuclear localization,[35,36] and the resultant effect of these multiple factors on HDAC translocation and transcription merits further study.

Higher quantitative effects in systems that are inherently integrative (like CaMKII activation and translocation) may be expected to recruit different qualitative responses such as CaT kinetics versus gene expression over time, depending upon extent and location of activation and kinetics of responses. Thus, we posit that the more limited, and kinetically reversible CaMKII activation at the perinuclear and SR domains may allow CaMKII to have beneficial adaptive effects on the amplitude and kinetics of CaTs to cause enhanced contraction to meet, in the case of TAC, a greater cardiac afterload. Indeed, CaMKII inhibition prevents the acute increase in CaTs in cells embedded in an afterload-inducing 3-dimensional gel.[37] However, as the extent of CaMKII activation gets stronger and more chronic (eg, by autophosphorylation, oxidation, or S-nitrosylation) inside the nucleus (rather than just around it) and reinforced by higher nuclear [Ca^{2+}], this can promote qualitative changes in gene transcription, assessed here by HDAC4 nuclear export and transcriptional activation of *TGF-β1*. And those changes in gene expression may undercut the short-term compensatory CaMKII effects on CaTs, which we know are lost in end-stage HF where SERCA function and CaTs are typically depressed.[2]

Gq-protein coupled receptors targeted by angiotensin II, endothelin-1, and α-adrenergic agonists tend to be activated as part of the neurohumoral storm associated with hypertrophic and HF signaling.[38] These agonists activate CaMKII and PKD (protein kinase D) and promote HDAC4/5 nuclear export. Part of this effect is caused by InsP$_3$ which promotes release of Ca^{2+} directly from the NE into the nucleoplasm and PN space.[16,39–41] We previously showed how the additional activation of nuclear InsP$_3$ receptors can greatly amplify the nuclear (and PN) Ca^{2+} signals induced by pacing, and that drive CaMKII activation, HDAC4 nuclear export, and hypertrophic gene signaling.[4] We speculate that the compensatory stage seen early in both TAC and CaMKIIδC-TG mice may provide adaptive advantage and that some tipping point is eventually reached, perhaps in response to elevated Gq-coupled receptor activation, that transitions the compensatory adaptive stage to one that is maladaptive in terms of both CaMKII activation levels and transcriptional signaling. Although this is an attractive hypothesis, understanding the impact of neurohormonal stimulation on perinuclear trafficking under a range of physiological pacing rates requires further investigation.

CaMKIIδC Versus CaMKIIδB in Driving Pathology

Experiments in myocytes from CaMKIIδC-TG mice in WT versus CaMKIIδ null background revealed that (1) the predominant splice variant responsible for the disproportionate P-CaMKII levels in the NE region is CaMKIIδC, and (2) the effect is not the result of higher CaMKIIδC expression, but rather redistribution of more active CaMKIIδC towards the nucleus and NE. Although CaMKII has been thought to be anchored in cardiomyocytes, Wood et al[7] demonstrated that CaMKII is highly mobile in adult ventricular myocytes even at rest and that its mobility is further enhanced by CaTs and its activation state.

To address downstream functional effects of perinuclear CaMKIIδC upregulation, we assessed HDAC4 translocation. Remarkably, overexpression of CaMKIIδC alone (KO-δCTG) induced baseline nuclear HDAC4 export even in the absence of CaMKIIδB. Moreover, the presence of CaMKIIδB in CaMKIIδC-TG mice (at the same overall level of CaMKIIδ and P-CaMKIIδ as in KO-δCTG; Figure III in the Data Supplement) did not cause net reduction in baseline nuclear HDAC4 export (based on F$_{Nuc}$/F$_{Cyto}$ in Figure 6B). Thus, CaMKIIδC strongly promotes HDAC4 to shift from nucleus to cytosol, and CaMKIIδB may limit that. In line with this hypothesis, we could show that in the absence of CaMKIIδC (ie, in CaMKIIδB transgenic mice in KO background), overexpression of CaMKIIδB, failed to exhibit similar effects on cardiac hypertrophy or function (Figure IX in the Data Supplement). Moreover, in line with more recent studies on CaMKIIδB mice, demonstrating that this nuclear splice variant exhibits cardioprotective effects,[8,42] we found a milder phenotype of CaMKIIδC-TG mice in WT versus in KO background, and in CaMKIIδC-TG mice in KO versus WT background (Figure 7 and Figure IX in the Data Supplement).

However, both TG mice showed reduced F$_{Nuc}$/F$_{PN}$ HDAC4 ratio at baseline versus WT, suggesting that both splice variants can influence baseline HDAC4

localization around the NE. In contrast, CaMKIIδ KO elevated nuclear-to-cytoplasmic HDAC4 ratio, confirming that baseline CaMKIIδ may suffice to drive some HDAC4 out of the nucleus. Importantly, the pacing-induced HDAC4 nuclear export was accelerated even in young asymptomatic CaMKIIδC-TG mice. Because it is well established that prolonged translocation of HDAC4 out of the nucleus relieves the suppression of hypertrophic gene programming leading to adverse cardiac phenotype,[18,33] this effect is expected to have pathological consequences.

Although no major cardiac dysfunction was seen in early (8 weeks) CaMKIIδC-TG mice, at 11 to 13 weeks, they exhibited massive hypertrophy and lung congestion (Figure 7A and 7B), major reductions in fractional shortening, and premature death.[13] To complement in vivo function measurements in TG[13] and KO-δCTG[8] mice, we also assessed cellular and nuclear dimensions in WT, KO, TG, and KO-δCTG mice. Although both CaMKIIδC transgenic mouse lines exhibited hypertrophic cardiac growth which progressed to HF, KO-δCTG mice showed accelerated remodeling as evidenced by more severe phenotypes at each stage. Also, the KO-δCTG mice displayed exclusively eccentric growth of both myocyte and nuclear length, whereas TG cardiomyocytes (with endogenous CaMKIIδB) showed more balanced concentric and eccentric growth, with preserved myocyte length/width ratio at the age of 6 to 8 weeks and only minimally increased at weeks 11 to 13 (Figure 7C through 7F). Those findings suggest that CaMKIIδC especially promotes eccentric cardiomyocyte growth, whereas CaMKIIδB may preferentially drive concentric hypertrophy or help to ensure balanced eccentric-concentric growth. This is a strong argument for a more deleterious role for CaMKIIδC versus CaMKIIδB in promoting adverse cardiac remodeling. This agrees with observations on the whole heart level, where CaMKIIδB-TG mice primarily develop cardiac hypertrophy whereas hypertrophy in the CaMKIIδC-TG mice is more dilated and rapidly transitions to HF.[18,43] In addition, Grey et al[8] observed that KO-δBTG mice had normal survival for at least 6 months, whereas KO-δCTG died prematurely with <20% survival by 21 weeks. Moreover, CaMKIIδB and δC variants had strikingly different effects on in vivo cardiac function; in 6- to 8-week-old KO-δCTG mice, fractional shortening was decreased by 63% compared to WT littermates while KO-δBTG mice showed no signs of cardiac dysfunction.

Human Data and Clinical Relevance

Our human HF data confirm the widely reported CaMKIIδ upregulation in human HF,[22,24,30] but here, we demonstrate that this is true also in the nuclear fraction and that the CaMKIIδC splice variant increases most dramatically. Thus, we conclude that the same pathological concentration of CaMKII to the nuclear domain that we

demonstrate in mouse is occurring in human HF as well, with the δC splice variant being the key culprit.

One caveat here is that while CaMKIIδB and δC (also known as δ_3 and δ_2, respectively) are major CaMKIIδ transcripts in mouse, Zhang et al[27] recently reported that a longer CaMKIIδ$_9$ mRNA product is especially prominent and pathological in humans. They found that CaMKIIδ$_9$ mRNA is expressed at levels similar to those of CaMKIIδB in mouse and human hearts and that CaMKIIδ$_9$ disrupts DNA repair causing genome instability and myocyte death. We cannot rule out that CaMKIIδ$_9$ expression contributes to the upper CaMKIIδ band (labeled δB in Figure 8C) because CaMKIIδ$_9$ protein is only 3 amino acids longer than δB. However, it is a less likely contaminant of the highly increased CaMKIIδ band labeled δC in Figure 8C since CaMKIIδ$_9$ is 14 amino acids longer than δC. The role of this isoform in perinuclear Ca signaling and HDAC redistribution merits future examination.

Taken together, our data indicate that increase in nuclear and perinuclear CaMKIIδC activation is a very early cellular response to pressure overload. Moreover, this CaMKII activation causes an adaptive compensatory TAC-induced enhancement of Ca^{2+} transients, as indicated by the finding that it is abolished acutely by CaMKII inhibition (Figure 1H). The concomitant enhancement of nuclear Ca^{2+} transients and time-averaged [Ca]$_{Nuc}$, in turn, further activate CaMKIIδC, causing its (peri)nuclear accumulation and HDAC4 nuclear export. Prolonged HDAC4 nuclear export likely promotes the hypertrophic gene program at the transcriptional level, and this may be amplified by CaMKIIδ-dependent phosphorylation at S10 on histone H3, which also occurs early in TAC.[44] This early phase of CaMKIIδ activation may indeed be beneficial and helps promote adaptive functional compensation, but in the long run, we hypothesize that this chronic CaMKII activation becomes a part of the maladaptive progression toward HF (including effects on Ca^{2+} handling, ion channels, inflammation, fibrosis, and interaction with other pathways). So, selective inhibition of CaMKIIδC (or δ$_9$) or HDAC nuclear export may be beneficial, especially in later HF stages.

Affiliations

Department of Cardiology (S.L.-H., N.D., J.V., M.A., I.M., M.S., S.R., M.W., D.v.L., S. Sedej) and Otto-Loewi Research Centre, Division of Pharmacology (M.H.), Medical University of Graz, Austria. Department of Pharmacology, University of California, Davis, CA (S.L.-H., A.W.H., S.M., B.M.W., J.B., D.M.B.). BioTechMed Graz, Austria (S.L.-H., J.V., S. Sedej). Klinik für Kardiologie und Pneumologie, Georg-August-Universität Göttingen, Germany (S. Sossalla). Klinik und Poliklinik für Innere Medizin II, Universitätsklinikum Regensburg, Germany (S.W., S. Sossalla). Institute for Medical Research, University of Belgrade, Serbia (M.I.). Department of Internal Medicine and Cardiology, Charité University Medicine Berlin, Germany (B.P.). Department of Pharmacology, University of California San Diego, La Jolla

Supplemental Materials

Expanded Materials and Methods
Online Tables I–V
Online Figures I–IX
References[45–50]

REFERENCES

1. Bers DM. Calcium cycling and signaling in cardiac myocytes. *Annu Rev Physiol*. 2008;70:23–49. doi: 10.1146/annurev.physiol.70.113006.100455
2. Lehnart SE, Maier LS, Hasenfuss G. Abnormalities of calcium metabolism and myocardial contractility depression in the failing heart. *Heart Fail Rev*. 2009;14:213–224. doi: 10.1007/s10741-009-9146-x
3. Kockskämper J, Seidlmayer L, Walther S, Hellenkamp K, Maier LS, Pieske B. Endothelin-1 enhances nuclear Ca^{2+} transients in atrial myocytes through Ins(1,4,5)P3-dependent Ca^{2+} release from perinuclear Ca^{2+} stores. *J Cell Sci*. 2008;121:186–195. doi: 10.1242/jcs.021386
4. Ljubojevic S, Radulovic S, Leitinger G, Sedej S, Sacherer M, Holzer M, Winkler C, Pritz E, Mittler T, Schmidt A, et al. Early remodeling of perinuclear Ca^{2+} stores and nucleoplasmic Ca^{2+} signaling during the development of hypertrophy and heart failure. *Circulation*. 2014;130:244–255. doi: 10.1161/CIRCULATIONAHA.114.008927
5. Anderson ME, Brown JH, Bers DM. CaMKII in myocardial hypertrophy and heart failure. *J Mol Cell Cardiol*. 2011;51:468–473. doi: 10.1016/j.yjmcc.2011.01.012
6. Mishra S, Gray CB, Miyamoto S, Bers DM, Brown JH. Location matters: clarifying the concept of nuclear and cytosolic CaMKII subtypes. *Circ Res*. 2011;109:1354–1362. doi: 10.1161/CIRCRESAHA.111.248401
7. Wood BM, Simon M, Galice S, Alim CC, Ferrero M, Pinna NN, Bers DM, Bossuyt J. Cardiac CaMKII activation promotes rapid translocation to its extra-dyadic targets. *J Mol Cell Cardiol*. 2018;125:18–28. doi: 10.1016/j.yjmcc.2018.10.010
8. Gray CB, Suetomi T, Xiang S, Mishra S, Blackwood EA, Glembotski CC, Miyamoto S, Westenbrink BD, Brown JH. CaMKIIδ subtypes differentially regulate infarct formation following ex vivo myocardial ischemia/reperfusion through NF-κB and TNF-α. *J Mol Cell Cardiol*. 2017;103:48–55. doi: 10.1016/j.yjmcc.2017.01.002
9. Ljubojević S, Bers DM. Measuring intranuclear and nuclear envelope Ca^{2+} vs. cytosolic Ca^{2+}. *Methods Mol Biol*. 2015;1234:135–147. doi: 10.1007/978-1-4939-1755-6_12
10. Ljubojević S, Walther S, Asgarzoei M, Sedej S, Pieske B, Kockskämper J. In situ calibration of nucleoplasmic versus cytoplasmic Ca^{2+} concentration in adult cardiomyocytes. *Biophys J*. 2011;100:2356–2366. doi: 10.1016/j.bpj.2011.03.060
11. Baier MJ, Klatt S, Hammer KP, Maier LS, Rokita AG. Ca^{2+}/calmodulin-dependent protein kinase II is essential in hyperacute pressure overload. *J Mol Cell Cardiol*. 2020;138:212–221. doi: 10.1016/j.yjmcc.2019.12.002
12. Maier LS, Zhang T, Chen L, DeSantiago J, Brown JH, Bers DM. Transgenic CaMKIIdeltaC overexpression uniquely alters cardiac myocyte Ca^{2+} handling: reduced SR Ca^{2+} load and activated SR Ca^{2+} release. *Circ Res*. 2003;92:904–911. doi: 10.1161/01.RES.0000069685.20258.F1
13. Zhang T, Maier LS, Dalton ND, Miyamoto S, Ross J Jr, Bers DM, Brown JH. The deltaC isoform of CaMKII is activated in cardiac hypertrophy and induces dilated cardiomyopathy and heart failure. *Circ Res*. 2003;92:912–919. doi: 10.1161/01.RES.0000069686.31472.C5
14. Edwards AG, Grandi E, Hake JE, Patel S, Li P, Miyamoto S, Omens JH, Heller Brown J, Bers DM, McCulloch AD. Nonequilibrium reactivation of Na$^+$ current drives early afterdepolarizations in mouse ventricle. *Circ Arrhythm Electrophysiol*. 2014;7:1205–1213. doi: 10.1161/CIRCEP.113.001666
15. Weiss JN, Karma A, MacLellan WR, Deng M, Rau CD, Rees CM, Wang J, Wisniewski N, Eskin E, Horvath S, et al. "Good enough solutions" and the genetics of complex diseases. *Circ Res*. 2012;111:493–504. doi: 10.1161/CIRCRESAHA.112.269084
16. Wu AZ, Xu D, Yang N, Lin SF, Chen PS, Cala SE, Chen Z. Phospholamban is concentrated in the nuclear envelope of cardiomyocytes and involved in perinuclear/nuclear calcium handling. *J Mol Cell Cardiol*. 2016;100:1–8. doi: 10.1016/j.yjmcc.2016.09.008
17. Erickson JR, Patel R, Ferguson A, Bossuyt J, Bers DM. Fluorescence resonance energy transfer-based sensor Camui provides new insight into mechanisms of calcium/calmodulin-dependent protein kinase II activation in intact cardiomyocytes. *Circ Res*. 2011;109:729–738. doi: 10.1161/CIRCRESAHA.111.247148
18. Zhang T, Kohlhaas M, Backs J, Mishra S, Phillips W, Dybkova N, Chang S, Ling H, Bers DM, Maier LS, et al. CaMKIIdelta isoforms differentially affect calcium handling but similarly regulate HDAC/MEF2 transcriptional responses. *J Biol Chem*. 2007;282:35078–35087. doi: 10.1074/jbc.M707083200
19. Wu X, Zhang T, Bossuyt J, Li X, McKinsey TA, Dedman JR, Olson EN, Chen J, Brown JH, Bers DM. Local InsP3-dependent perinuclear Ca^{2+} signaling in cardiac myocyte excitation-transcription coupling. *J Clin Invest*. 2006;116:675–682. doi: 10.1172/JCI27374
20. Koitabashi N, Danner T, Zaiman AL, Pinto YM, Rowell J, Mankowski J, Zhang D, Nakamura T, Takimoto E, Kass DA. Pivotal role of cardiomyocyte TGF-β signaling in the murine pathological response to sustained pressure overload. *J Clin Invest*. 2011;121:2301–2312. doi: 10.1172/JCI44824
21. Suetomi T, Willeford A, Brand CS, Cho Y, Ross RS, Miyamoto S, Brown JH. Inflammation and NLRP3 inflammasome activation initiated in response to pressure overload by Ca^{2+}/Calmodulin-dependent protein kinase II δ signaling in cardiomyocytes are essential for adverse cardiac remodeling. *Circulation*. 2018;138:2530–2544. doi: 10.1161/CIRCULATIONAHA.118.034621
22. Ai X, Curran JW, Shannon TR, Bers DM, Pogwizd SM. Ca^{2+}/calmodulin-dependent protein kinase modulates cardiac ryanodine receptor phosphorylation and sarcoplasmic reticulum Ca^{2+} leak in heart failure. *Circ Res*. 2005;97:1314–1322. doi: 10.1161/01.RES.0000194329.41863.89
23. Bossuyt J, Helmstadter K, Wu X, Clements-Jewery H, Haworth RS, Avkiran M, Martin JL, Pogwizd SM, Bers DM. Ca^{2+}/calmodulin-dependent protein kinase IIdelta and protein kinase D overexpression reinforce the histone deacetylase 5 redistribution in heart failure. *Circ Res*. 2008;102:695–702. doi: 10.1161/CIRCRESAHA.107.169755
24. Hoch B, Meyer R, Hetzer R, Krause EG, Karczewski P. Identification and expression of delta-isoforms of the multifunctional Ca^{2+}/calmodulin-dependent protein kinase in failing and nonfailing human myocardium. *Circ Res*. 1999;84:713–721. doi: 10.1161/01.res.84.6.713
25. Sossalla S, Fluschnik N, Schotola H, Ort KR, Neef S, Schulte T, Wittköpper K, Renner A, Schmitto JD, Gummert J, et al. Inhibition of elevated Ca^{2+}/calmodulin-dependent protein kinase II improves contractility in human failing myocardium. *Circ Res*. 2010;107:1150–1161. doi: 10.1161/CIRCRESAHA.110.220418
26. Erickson JR, Pereira L, Wang L, Han G, Ferguson A, Dao K, Copeland RJ, Despa F, Hart GW, Ripplinger CM, et al. Diabetic hyperglycaemia activates CaMKII and arrhythmias by O-linked glycosylation. *Nature*. 2013;502:372–376. doi: 10.1038/nature12537
27. Zhang M, Gao H, Liu D, Zhong X, Shi X, Yu P, Jin L, Liu Y, Tang Y, Song Y, et al. CaMKII-δ9 promotes cardiomyopathy through disrupting UBE2T-dependent DNA repair. *Nat Cell Biol*. 2019;21:1152–1163. doi: 10.1038/s41556-019-0380-8
28. Ling H, Zhang T, Pereira L, Means CK, Cheng H, Gu Y, Dalton ND, Peterson KL, Chen J, Bers D, et al. Requirement for Ca^{2+}/calmodulin-dependent kinase II in the transition from pressure overload-induced cardiac hypertrophy to heart failure in mice. *J Clin Invest*. 2009;119:1230–1240. doi: 10.1172/JCI38022
29. Toischer K, Rokita AG, Unsöld B, Zhu W, Kararigas G, Sossalla S, Reuter SP, Becker A, Teucher N, Seidler T, et al. Differential cardiac remodeling in preload versus afterload. *Circulation*. 2010;122:993–1003. doi: 10.1161/CIRCULATIONAHA.110.943431
30. Fischer TH, Eiringhaus J, Dybkova N, Förster A, Herting J, Kleinwächter A, Ljubojevic S, Schmitto JD, Streckfuß-Bömeke K, Renner A, et al. Ca^{2+}/calmodulin-dependent protein kinase II equally induces sarcoplasmic reticulum Ca^{2+} leak in human ischaemic and dilated cardiomyopathy. *Eur J Heart Fail*. 2014;16:1292–1300. doi: 10.1002/ejhf.163

31. Hegyi B, Bossuyt J, Ginsburg KS, Mendoza LM, Talken L, Ferrier WT, Pogwizd SM, Izu LT, Chen-Izu Y, Bers DM. Altered repolarization reserve in failing rabbit ventricular myocytes: calcium and beta-adrenergic effects on delayed- and inward-rectifier potassium currents. *Circ Arrhythm Electrophysiol*. 2018;11:e005852.

32. Nakagawa T, Yokoe S, Asahi M. Phospholamban degradation is induced by phosphorylation-mediated ubiquitination and inhibited by interaction with cardiac type Sarco(endo)plasmic reticulum Ca^{2+}-ATPase. *Biochem Biophys Res Commun*. 2016;472:523–530. doi: 10.1016/j.bbrc.2016.03.009

33. Backs J, Olson EN. Control of cardiac growth by histone acetylation/deacetylation. *Circ Res*. 2006;98:15–24. doi: 10.1161/01.RES.0000197782.21444.8f

34. Dodge-Kafka K, Gildart M, Tokarski K, Kapiloff MS. mAKAPβ signalosomes - A nodal regulator of gene transcription associated with pathological cardiac remodeling. *Cell Signal*. 2019;63:109357. doi: 10.1016/j.cellsig.2019.109357

35. Backs J, Worst BC, Lehmann LH, Patrick DM, Jebessa Z, Kreusser MM, Sun Q, Chen L, Heft C, Katus HA, et al. Selective repression of MEF2 activity by PKA-dependent proteolysis of HDAC4. *J Cell Biol*. 2011;195:403–415. doi: 10.1083/jcb.201105063

36. Chang CW, Lee L, Yu D, Dao K, Bossuyt J, Bers DM. Acute β-adrenergic activation triggers nuclear import of histone deacetylase 5 and delays G(q)-induced transcriptional activation. *J Biol Chem*. 2013;288:192–204. doi: 10.1074/jbc.M112.382358

37. Jian Z, Han H, Zhang T, Puglisi J, Izu LT, Shaw JA, Onofiok E, Erickson JR, Chen YJ, Horvath B, et al. Mechanochemotransduction during cardiomyocyte contraction is mediated by localized nitric oxide signaling. *Sci Signal*. 2014;7:ra27. doi: 10.1126/scisignal.2005046

38. Drawnel FM, Archer CR, Roderick HL. The role of the paracrine/autocrine mediator endothelin-1 in regulation of cardiac contractility and growth. *Br J Pharmacol*. 2013;168:296–317. doi: 10.1111/j.1476-5381.2012.02195.x

39. Archer CR, Robinson EL, Drawnel FM, Roderick HL. Endothelin-1 promotes hypertrophic remodelling of cardiac myocytes by activating sustained signalling and transcription downstream of endothelin type A receptors. *Cell Signal*. 2017;36:240–254. doi: 10.1016/j.cellsig.2017.04.010

40. Hohendanner F, Maxwell JT, Blatter LA. Cytosolic and nuclear calcium signaling in atrial myocytes: IP3-mediated calcium release and the role of mitochondria. *Channels (Austin)*. 2015;9:129–138. doi: 10.1080/19336950.2015.1040966

41. Zima AV, Bare DJ, Mignery GA, Blatter LA. IP3-dependent nuclear Ca^{2+} signalling in the mammalian heart. *J Physiol*. 2007;584:601–611. doi: 10.1113/jphysiol.2007.140731

42. Little GH, Saw A, Bai Y, Dow J, Marjoram P, Simkhovich B, Leeka J, Kedes L, Kloner RA, Poizat C. Critical role of nuclear calcium/calmodulin-dependent protein kinase IIdeltaB in cardiomyocyte survival in cardiomyopathy. *J Biol Chem*. 2009;284:24857–24868. doi: 10.1074/jbc.M109.003186

43. Gray CB, Heller Brown J. CaMKIIdelta subtypes: localization and function. *Front Pharmacol*. 2014;5:15. doi: 10.3389/fphar.2014.00015

44. Awad S, Al-Haffar KM, Marashly Q, Quijada P, Kunhi M, Al-Yacoub N, Wade FS, Mohammed SF, Al-Dayel F, Sutherland G, et al. Control of histone H3 phosphorylation by CaMKIIδ in response to haemodynamic cardiac stress. *J Pathol*. 2015;235:606–618. doi: 10.1002/path.4489

45. Sedej S, Schmidt A, Denegri M, Walther S, Matovina M, Arnstein G, Gutschi EM, Windhager I, Ljubojevic S, Negri S, et al. Subclinical abnormalities in sarcoplasmic reticulum Ca^{2+} release promote eccentric myocardial remodeling and pump failure death in response to pressure overload. *J Am Coll Cardiol*. 2014;63:1569–1579. doi: 10.1016/j.jacc.2013.11.010

46. Sedej S, Heinzel FR, Walther S, Dybkova N, Wakula P, Groborz J, Gronau P, Maier LS, Vos MA, Lai FA, et al. Na$^+$-dependent SR Ca^{2+} overload induces arrhythmogenic events in mouse cardiomyocytes with a human CPVT mutation. *Cardiovasc Res*. 2010;87:50–59. doi: 10.1093/cvr/cvq007

47. Pogwizd SM, Qi M, Yuan W, Samarel AM, Bers DM. Upregulation of Na$^+$/Ca^{2+} exchanger expression and function in an arrhythmogenic rabbit model of heart failure. *Circ Res*. 1999;85:1009–1019. doi: 10.1161/01.RES.85.11.1009

48. Djalinac N, Ljubojevic-Holzer S, Matzer I, Kolesnik E, Jandl K, Lohberger B, Rainer P, Heinemann A, Sedej S, von Lewinski D, et al. The role of stretch, tachycardia and sodium-calcium exchanger in induction of early cardiac remodelling. *J Cell Mol Med*. 2020;24:8732–8743. doi: 10.1111/jcmm.15504

49. Huke S, Bers DM. Temporal dissociation of frequency-dependent acceleration of relaxation and protein phosphorylation by CaMKII. *J Mol Cell Cardiol*. 2007;42:590–599. doi: 10.1016/j.yjmcc.2006.12.007

50. Shaiken TE, Opekun AR. Dissecting the cell to nucleus, perinucleus and cytosol. *Sci Rep*. 2014;4:4923. doi: 10.1038/srep0492